

---

Masters Theses

Student Theses and Dissertations

---

Summer 2010

## Sintering and microstructural effects on mechanical properties of zirconium carbide-tungsten cermets

Melissa M. Giles Craft

Follow this and additional works at: [https://scholarsmine.mst.edu/masters\\_theses](https://scholarsmine.mst.edu/masters_theses)



Part of the [Ceramic Materials Commons](#)

Department:

---

### Recommended Citation

Craft, Melissa M. Giles, "Sintering and microstructural effects on mechanical properties of zirconium carbide-tungsten cermets" (2010). *Masters Theses*. 117.

[https://scholarsmine.mst.edu/masters\\_theses/117](https://scholarsmine.mst.edu/masters_theses/117)

This thesis is brought to you by Scholars' Mine, a service of the Missouri S&T Library and Learning Resources. This work is protected by U. S. Copyright Law. Unauthorized use including reproduction for redistribution requires the permission of the copyright holder. For more information, please contact [scholarsmine@mst.edu](mailto:scholarsmine@mst.edu).

SINTERING AND MICROSTRUCTURAL EFFECTS ON MECHANICAL  
PROPERTIES OF ZIRCONIUM CARBIDE-TUNGSTEN CERMETS

by

MELISSA MARIE GILES CRAFT

A THESIS

Presented to the Faculty of the Graduate School of the  
MISSOURI UNIVERSITY OF SCIENCE AND TECHNOLOGY

In Partial Fulfillment of the Requirements for the Degree

MASTER OF SCIENCE IN CERAMIC ENGINEERING

2010

Approved by

William G. Fahrenholtz, Advisor

Gregory E. Hilmas

Jeffrey D. Smith



## **PUBLICATION THESIS OPTION**

Introduction and Background sections provide information about the thesis topic. Paper I is the manuscript titled “Microstructure and mechanical properties of ZrC-W cermets” planned for submission to Materials Science and Engineering A. Paper II is the manuscript titled “Densification and Microstructure of ZrC-W Cermets” planned for submission to Ceramics International.

## ABSTRACT

Zirconium carbide-tungsten cermets were prepared by in situ reaction sintering a mixture of zirconia and tungsten carbide. Tungsten is a refractory metal with a melting point of 3422°C; however, its mechanical strength decreases significantly with increasing temperature. One approach to improve the elevated temperature strength is to add ceramic particulates to the matrix. Zirconia and tungsten carbide were compacted and then reacted and sintered in a single step by heating to 2050°C. The resulting stoichiometric zirconium carbide-tungsten cermet had a relative density greater than 96%. Cermets with two different grain sizes were produced by altering the final sintering temperature. Sintering at 2050°C resulted in features measuring  $< 1 \mu\text{m}$  and a strength of 530 MPa, compared to sintering at 2100°C which resulted in features measuring  $> 2 \mu\text{m}$  and a strength measuring 450 MPa. Cermets with different ZrC:W ratios were also evaluated. Composites containing 35, 50 and 65 vol% ZrC were prepared and tested for hardness, with values ranging from 9 GPa to 13 GPa for materials containing 35 vol% and 65 vol% ZrC, respectively. The cermets were also prepared by hot pressing. The hot pressed samples were used as a comparison of properties and microstructure. The effects of the composition and microstructure on the mechanical properties were evaluated.

## ACKNOWLEDGMENTS

Many thanks to my advisor, Dr. Fahrenholtz, for taking a chance on me and helping me get adjusted to the materials field. His knowledge, patience and support have helped me achieve my goal. I would also like to thank Dr. Hilmas for his guidance through the materials testing portion of my research. Also, the excellent instruction I received in my coursework is invaluable to me and also greatly appreciated.

I would like to extend my appreciation to the UHTC group, without their guidance on the processing and testing of the materials I would not have gotten as far as I did. I would especially like to thank Sumin Zhu, Jeremy Watts, Matt Thompson, Harlan Brown-Shaklee and Dr. Zhang for coming to my aid when things went wrong, which they inevitably did.

Thanks to Eric Bohannon for his assistance in XRD analysis as well as assisting me in the understanding and use of the lattice parameters.

I would like to extend my appreciation to the undergraduates that helped me complete my work. Jon Bock, for his excellent use of the attrition mill, and David Shahin, whose assistance with the materials processing and the characterization, especially SEM imaging, were invaluable to this research.

I would like to thank my husband whose patience, love and support have helped me get through the tough times and celebrated with me in the times of success.

Finally, I would like to thank all my friends and family for their love and support in my crazy adventure. Without their support and guidance I would not have made it to the end of my academic career and to the start of the rest of my life.

## TABLE OF CONTENTS

	Page
PUBLICATION THESIS OPTION.....	iii
ABSTRACT .....	iv
ACKNOWLEDGMENTS .....	v
LIST OF ILLUSTRATIONS.....	viii
LIST OF TABLES .....	x
SECTION	
1. INTRODUCTION.....	1
1.1. PURPOSE.....	1
1.2. REFERENCES .....	3
2. BACKGROUND.....	5
2.1. TUNGSTEN .....	7
2.2. ZIRCONIUM CARBIDE .....	10
2.3. ZIRCONIUM CARBIDE – TUNGSTEN CERMETS.....	13
2.4. PROCESSING METHODS .....	17
2.4.1. Conventional Hot Pressing .....	18
2.4.2. In Situ Reaction Sintering .....	19
2.5. REFERENCES .....	20
PAPER	
I. MICROSTRUCTURE AND MECHANICAL PROPERTIES OF ZrC-W CERMETS.....	24
1.1 ABSTRACT .....	24
1.2 INTRODUCTION .....	24
1.3 EXPERIMENTAL PROCEDURE .....	27
1.3.1 Processing .....	27
1.3.2 Characterization .....	29
1.3.3 Mechanical Testing .....	30
1.4 RESULTS AND DISCUSSION.....	31
1.5 CONCLUSIONS.....	44

1.6 REFERENCES .....	45
II. DENSIFICATION AND MICROSTRUCTURE OF ZrC-W CERMETS .....	47
2.1 ABSTRACT .....	47
2.2 INTRODUCTION .....	47
2.3 EXPERIMENTAL PROCEDURE .....	50
2.3.1 In Situ Reaction Sintering .....	50
2.3.2 Hot Pressing .....	53
2.3.3 Characterization and Testing .....	54
2.4 RESULTS AND DISCUSSION .....	56
2.4.1 Thermodynamic Considerations .....	56
2.4.2 Densification .....	61
2.4.3 SEM Analysis .....	63
2.4.4 Hardness .....	67
2.5 CONCLUSIONS .....	69
2.6 REFERENCES .....	70
SECTION	
3. CONCLUSION .....	72
4. SUGGESTIONS FOR FUTURE WORK .....	74
APPENDIX .....	76
VITA .....	78

## LIST OF ILLUSTRATIONS

	Page
Figure 2-1: Temperature dependence of the hardness of W. ....	9
Figure 2-2: Temperature dependence of the strength of W. ....	9
Figure 2-3: Temperature dependence of the tensile strength of different W alloys compared to monolithic W. ....	10
Figure 2-4: Zr-C phase diagram. ....	13
 Paper I	
Figure 1-1: Pellets before and after in situ reaction sintering. ....	32
Figure 1-2: XRD patterns for the unreacted starting powders and materials that were reaction sintered at various temperatures. ....	33
Figure 1-3: ZrC-W phase diagram. ....	35
Figure 1-4: XRD spectra of the materials that were hot-pressed at 2050°C and 32MPa. ....	36
Figure 1-5: Relative density as a function of processing temperature for ZrC-W cermets prepared by in situ reaction sintering (closed squares) and conventional hot pressing (closed triangles). ....	37
Figure 1-6: SEM images of the polished surfaces of ZrC-W cermets produced by in situ reaction sintering at different temperatures. ....	39
Figure 1-7: SEM micrograph of a ground and polished surface of 35 vol% ZrC, 65 vol% W cermet produced by hot pressing. ....	41
 Paper II	
Figure 2-1: Phenolic resin charring schedule. ....	52
Figure 2-2: Standard state change in Gibbs free energy ( $\Delta G_{rxn}^{\circ}$ ) for Reactions 1, 2, and 3. ....	58
Figure 2-3 XRD patterns for specimens produced by in situ reaction sintering (Rxn) or hot pressing (HP) at various temperatures. ....	60
Figure 2-4: Relative density as a function of sintering or hot pressing temperature. ....	63

Figure 2-5: SEM micrographs comparing the microstructure of reaction sintered specimens of varying ZrC content a) 35 vol% ZrC (2050°C), b) 50 vol% ZrC (2100°C), c) 65 vol% ZrC (2000°C). .....	64
Figure 2-6: SEM microstructure of reaction 2-3 cross section. ....	65
Figure 2-7: SEM micrographs comparing the microstructure of hot pressed specimens of varying ZrC additions a) 35 vol% ZrC (2050°C 32 MPa), b) 50 vol% ZrC (1900°C 32 MPa), c) 65 vol% ZrC (1800°C 32 MPa). .....	66
Figure 2-8: Hardness in relation to ZrC content. ....	69

## LIST OF TABLES

	Page
Table 2-1: Mechanical properties tested at room temperature for ZrC-W cermets. ....	16
Paper I	
Table 1-1: Lattice parameter measurements as determined from XRD analysis along with the calculated amounts W in solid solution.....	34
Table 1-2: Compositions predicted by analysis of SEM micrographs and the amount of porosity. ....	40
Table 1-3: Mechanical properties of ZrC-W cermets made by both pressureless reaction sintering and hot pressing.....	43
Table 1-4: Calculated critical flaw size for reaction sintered materials. ....	44
Paper II	
Table 2-1: The values of $x$ for Reactions 2-2 and 2-3, and the corresponding amounts of phenolic resin added along with the predicted carbon yield. ....	52
Table 2-2: Density comparison for the three different compositions for in situ reaction sintered (Rxn) and hot-pressed (HP) samples. ....	54
Table 2-3: Predicted reaction temperatures for under vacuum and at atmospheric pressure of Reactions 2-1, 2-2, and 2-3.....	58
Table 2-4 Lattice parameters of ZrC and the corresponding amount of W in solid solution (ss) for the highest density samples both produced by in situ reaction sintering (Rxn) and hot pressing (HP). ....	61
Table 2-5: Feature size analysis. ....	67
Table 2-6: Hardness. ....	67



## SECTION

### 1. INTRODUCTION

#### 1.1. PURPOSE

The goal of this work is to study the microstructure and properties of zirconium carbide-tungsten (ZrC-W) cermets prepared using different metal to ceramic ratios, processing conditions and processing methods. Cermets, such as ZrC-W, are of interest because of potential uses in ultra high temperature applications. The cermets offer the potential for improved properties and enhanced performance for components typically made from tungsten or tungsten alloys. One potential application is solid-fueled rocket nozzles. Currently these nozzles are made of tungsten or a low alloy tungsten such as W-Re [1]. However, these materials have high failure rates in the harsh environments and can be limited to one time use [2]. When exposed to a flame containing molten alumina, tungsten experienced limited oxidation, but had significant material loss by cavitation, caused from the collapse of small clouds of alumina vapor [3]. To overcome some of the limitations associated with pure tungsten, the metal is often alloyed with other refractory metals such as Re or is reinforced by a second phase such as HfC, La<sub>2</sub>O<sub>3</sub>, ThO<sub>2</sub>, ZrC, TiC, or Ta<sub>2</sub>C. Carbides are also useful in high-temperature applications since many of them, like W, have ultra-high melting points above 3000°C. Also, carbides such as ZrC and TiC have been shown to improve the ablation properties of W [4,5]. ZrC is the material of choice for this study because of its high melting point, as well as its similar thermal and mechanical properties to W. For example, the thermal expansion coefficient of ZrC is  $4.0 \times 10^{-6}/^{\circ}\text{C}$  compared to  $4.5 \times 10^{-6}/^{\circ}\text{C}$  for W at room temperature [4]. ZrC also

has high corrosion resistance [6], being able to be heated to the melting point in hydrogen without decomposition [7]. Oxidation of ZrC occurs in air at and above 800°C [7]. However, it does dissolve in cold HNO<sub>3</sub> as well as a mixture of H<sub>2</sub>SO<sub>4</sub> and H<sub>3</sub>PO<sub>4</sub> [7]. ZrC has been shown to be compatible with W forming a solid solution in both phases [8] as well as having a similar coefficient of thermal expansion [4], which allows heating to elevated temperatures without cracking.

Several different processing techniques have been used to produce these materials and all offer the potential for controlling the metal to ceramic ratio and microstructure, which can lead to control over the properties. Ideally, the individual desirable properties of ZrC and W will both contribute to the final properties of the cermet. ZrC has better ablation resistance increasing the ablation rate for W-ZrC to  $3.28 \times 10^{-3}$  mm/s at 2500°C compared to  $1.49 \times 10^{-2}$  mm/s for W [2] and higher hardness (25.5 GPa) [7] than W (3.4 GPa) [9], whereas W is more ductile than, which may improve the fracture toughness of the cermet compared to a monolithic ceramic ( $7.6 \text{ MPa m}^{1/2}$  for monolithic W) [10]. The two materials both have high melting temperatures, 3422°C for W and 3445°C for ZrC [11]. These individual properties, when combined in a cermet, have the potential to provide superior properties for many applications compared to the individual materials.

As part of this study, two different processing methods, conventional hot pressing and in situ reaction sintering [12,13], were used to produce specimens that were near full density. The difference between these processing methods leads to differences in microstructure and properties of the resulting cermets. While it may seem like one method is better in regards to some properties, both methods have benefits and limitations. In addition, it was discovered that these materials exhibit rapid grain

coarsening at temperatures between 2050°C and 2100°C, but can be densified at either temperature. This allows for control over the size of the microstructure, but also allows for the ability to vary the resulting mechanical properties. The purpose of this research is to investigate multiple methods of producing ZrC-W cermets and compare the characteristics and mechanical properties of the resulting specimens.

## 1.2. REFERENCES

- [1] E. Lassner, W. D. Schubert, Tungsten: Properties, Chemistry, Technology of the Element, Alloys, and Chemical Compounds, Plenum Publishers, New York, 1999.
- [2] M. C. Teague, G. E. Hilmas, W. G. Fahrenholtz, "Reaction processing of ultra-high temperature W/Ta<sub>2</sub>C-based cermets," *J. Am. Ceram. Soc.* 92[9] (2009) 1966-1971.
- [3] A. G. Metcalfe, N. B. Elsner, E. Wuchina, M. Opeka, "Oxidation above 3300°C of refractory materials in an aluminized flame," *Proceedings—Electrochemical Society 2003-16 (High Temperature Corrosion and Materials Chemistry IV)*, Paris, France, 2003 pp. 420-30.
- [4] M. B. Dickerson, P. J. Wurm, J. R. Schorr, W. P. Hoffman, P. G. Wapner, and K. H. Sandhage, "Near net-shape, ultra-high melting, recession-resistant ZrC/W-based rocket nozzle liners via the displacive compensation of porosity (DCP) method," *J. Mat. Sci.* 39 (2004) 6005-6015.
- [5] G. M. Song, Y. Zhou, Y. J. Wang, "Effect of carbide particles on the ablation properties of tungsten composites," *Mater. Character.* 50 (2003) 293-303.
- [6] X.M. He and L. Shu, "High corrosion resistant ZrC films synthesized by ion-beam assisted deposition," *J. of Mater. Res.* 14 (1999) 615-618.
- [7] H. O. Pierson, *Handbook of Refractory Carbides and Nitrides*, Noyes Publications, Westwood, NJ, 1996 pp. 74.
- [8] A. E. McHale (ed.) *Phase Diagrams for Ceramists*, Vol. X. American Ceramic Society, Westerville, OH, 1994, pp. 371.
- [9] G. M. Song, Y.J. Wang and Y. Zhou, "Elevated temperature ablation resistance and Thermophysical properties of tungsten matrix composites reinforced with ZrC particles," *J. Mat. Sci.* 36, 4625-4631, (2001).

- [10] G. M. Song, Y. J. Wang, and Y. Zhou, "The Mechanical and Thermophysical Properties of ZrC/W Composites at Elevated Temperature," *Mater. Sci. Eng. A*, 334 (2002) 223-32.
- [11] E. Rudy, *Compendium of Phase Diagram Data*, Air Force Materials Laboratory Metals and Ceramics Division, Wright-Patterson AFB, OH, 1969, pp. 162.
- [12] S. C. Zhang, G. E. Hilmas, W. G. Fahrenholtz. "Zirconium Carbide-Tungsten Cermets Prepared by In Situ Reaction Sintering," *J. Am. Ceram. Soc.*, 90 [6] (2007) 1930-1933.
- [13] S. C. Zhang, G. E. Hilmas, W. G. Fahrenholtz, US patent 7 648 675, 19 January 2010.

## 2. BACKGROUND

Materials are an enabling factor in the advancement of technology [1]. This is especially true for high temperature applications. Materials such as refractory metals and ultra-high temperature ceramics (UHTCs) are an option for operating continuously at temperatures of 1600°C or higher. Operating temperatures in this range often require materials that have melting points in excess of 3000°C. These materials also need to retain strength at elevated temperatures, maintain corrosion resistance, and have a low coefficient of thermal expansion. An example of a refractory metal in a high temperature application is tungsten (W) used for rocket nozzles, advancements in materials are looked to because, W loses 60% of the room temperature strength above 1000°C [2], W nozzles have also seen major pitting assumed to be from cavitation caused by the collapse of alumina vapor clouds [3]. Additionally, low coefficients of thermal expansion are needed to reduce stresses caused by rapid changes in temperature during operation. The build up of stresses due to temperature changes can cause cracking. Cracking is minimized by using low CTE materials. To meet future needs, materials can be engineered to offer the desired properties. Cermets are an area of interest since they have the potential to combine the unique properties of ceramics, such as high hardness and melting temperatures, with the ductility and fracture toughness of metals.

Refractory metals and high temperature ceramics are ideal for forming high temperature cermets. The ceramic phase should provide stiffness, which will reduce deformation from creep allowing the part to maintain its shape and strength with increasing temperature. The metal increases the fracture toughness. It is important that

the cermet components do not react with each other at elevated temperatures; however, it has been shown that some solid solution at interfaces increases the strength of the bonding between the two phases, which can improve strength and fracture toughness [4]. Ideally no reaction will take place after the final processing. The materials of interest for this study are zirconium carbide (ZrC) as the ceramic component and tungsten (W) as the metal component. ZrC and W are chemically and mechanically compatible and have shown chemical stability at elevated temperatures both in theoretical and in experimental studies [5].

Most commonly, ZrC-W cermets have been produced by conventional hot pressing of ZrC and W powders [6,7]. Recent work has shown a new method of in situ reaction sintering that has produced near full density materials [8,9]. Hot pressing and in situ reaction sintering methods of fabrication both have benefits. Hot pressing often produces materials that are near theoretical density and stronger. Hot pressing produces potentially stronger materials by two methods; by having fewer and smaller pores at higher densities, the largest flaw is reduced thus improving strength also by sintering at lower temperatures, made possible by the applied pressure the grain sizes are reduced as well. Reaction sintering allows for near net shape production that reduces total time required to fabricate a finished component. In addition, reaction sintering typically allows the use of less costly starting materials such as oxides which are typically easier to produce.

The next three sections discuss in detail the materials used in this work, including tungsten, zirconium carbide, and ZrC-W cermets. This is followed by a detailed description of the various processing methods used in this work, including hot pressing

and pressureless sintering as well as other fabrication techniques that have been used in previous work.

## 2.1. TUNGSTEN

Tungsten is known for being the highest melting temperature refractory metal, with a melting point of 3410°C [10]. Because of the high melting temperature, tungsten is one of the most extensively used refractory metals for high temperature applications. Currently tungsten and its alloys are being used in rocket nozzles, ignition tubes, construction materials in nuclear reactors, in fusion reactors like the International Thermonuclear Experimental Reactor (ITER), and shielding material for space fission power systems [11,12]. When alloyed, tungsten has high erosion resistance, good thermal shock resistance, and good thermal conductivity [11].

The mechanical properties of tungsten at room temperature are attractive. With a room temperature strength of 705 MPa, a hardness of 3.4 GPa and an elastic modulus of 313 GPa, it is suitable for many applications. However, for unalloyed W, the hardness and strength drop drastically with increasing temperature [12]. Figure 2-1 shows that hardness decreases from nearly 450 HV (4.4 GPa) at room temperature to ~10 HV (0.1 GPa) above 2500°C [12]. Figure 2-2 shows that strength drops from ~400 MPa at room temperature to ~50 MPa above 400°C [12]. Another study showed that the decrease in strength was roughly 60% from room temperature to 1000°C [2]. Tungsten alloys have tensile strengths at room temperature ranging from 870-1000 MPa and elastic moduli of 350 to 400 GPa [6,12] and show promise for maintaining their strength at elevated

temperatures, with the addition of 30 vol% ZrC additions to tungsten the maximum strength is reached at 1000°C [6].

When it is alloyed with rhenium (Re), tungsten exhibits a lower ductile to brittle transformation temperature (DBTT), as well as an increase in workability. Pure tungsten has a DBTT of 400°C. By adding Re, the DBTT has been reduced to below room temperature. However, in some alloy amounts, the workability and high temperature strength are still limited; thus additional alloying elements such as carbon, Mo, Zr, Hf, Ti are added to maintain these properties [2]. Adding ceramic particles, in addition to Re, increases the high temperature strength better than alloying with only Re (Figure 2-3). Thoria ( $\text{ThO}_2$ ) has been an oxide of interest because it has one of the highest melting points of the oxides [13]. The addition of refractory carbides such as HfC, TiC and ZrC can also improve the high temperature strength of tungsten [14]. Ceramics have a lower density than tungsten and thus result in a lighter material than tungsten, whereas Re has a higher density at  $22 \text{ g/cm}^3$  [15]. Tungsten has many desired properties, but lacks certain properties needed for high temperature applications such as, high temperature strength, which can be improved by the addition of ceramics like ZrC.



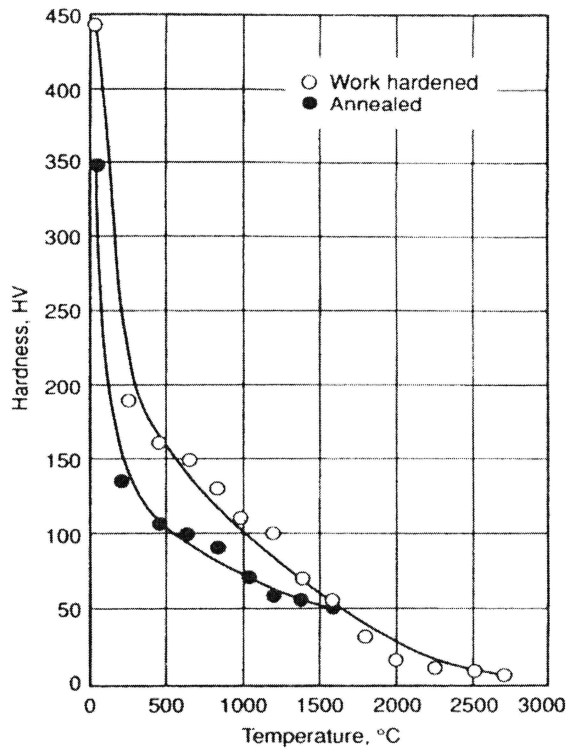


Figure 2-1: Temperature dependence of the hardness of W [12].

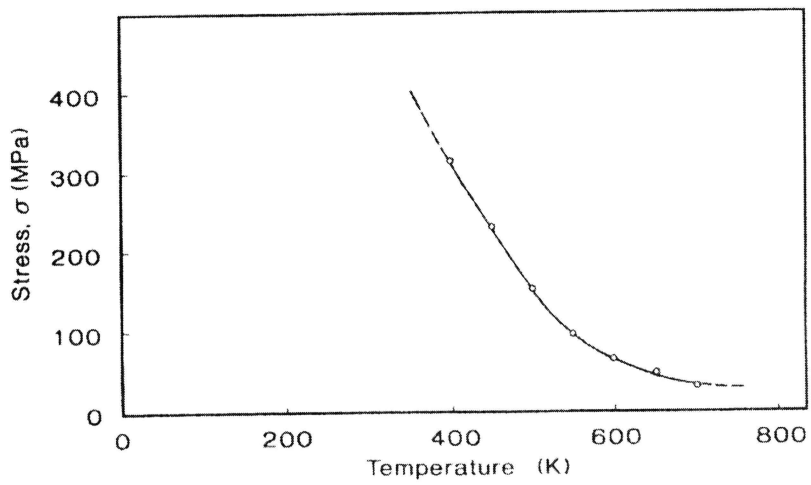


Figure 2-2: Temperature dependence of the strength of W [12].

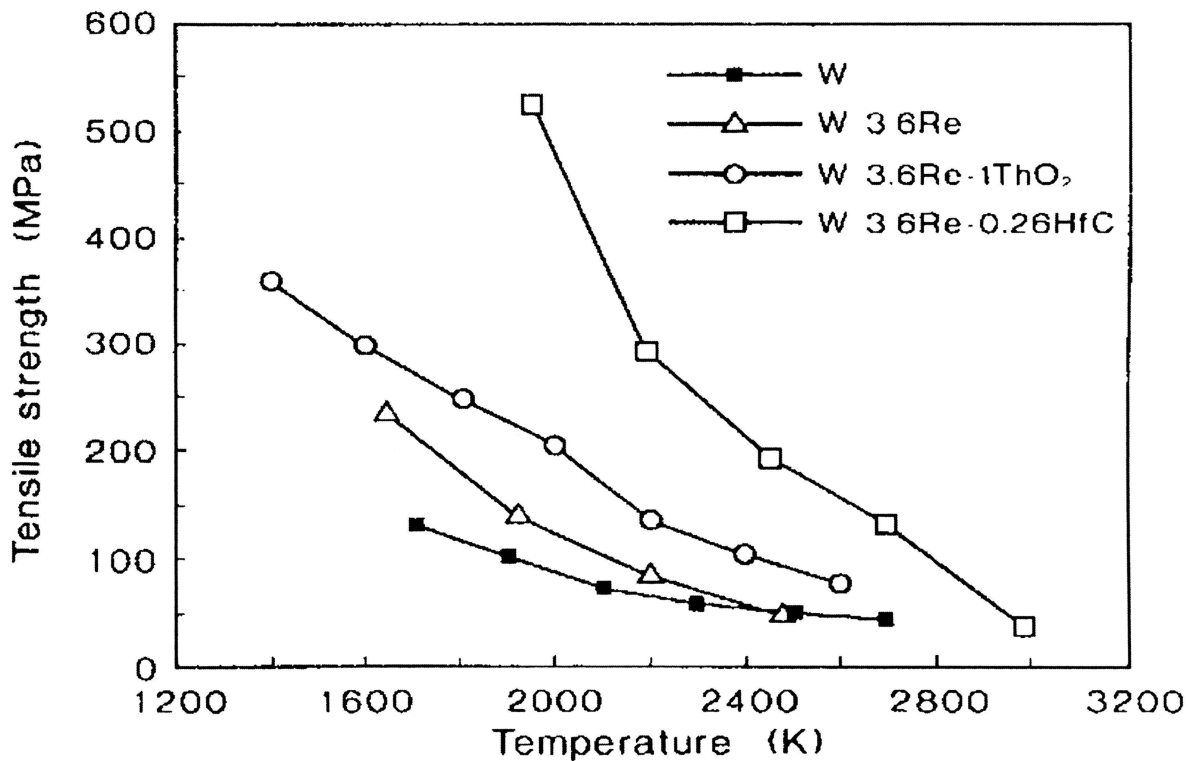


Figure 2-3: Temperature dependence of the tensile strength of different W alloys compared to monolithic W [12].

## 2.2. ZIRCONIUM CARBIDE

Zirconium carbide is known in particular for its chemical resistance and high temperature mechanical and thermal properties. High hardness (20 GPa), high elastic modulus (392 GPa), and high melting temperature (3445°C) make this material ideal for high temperature applications [16,19]. ZrC is also under consideration for applications in nuclear reactors because of the high melting point it is a candidate for replacing SiC in inert matrix fuels for very high temperature reactors [17,18].

Early research on ZrC was performed in the 1950-1970's when advancements for military applications were the driving factor for discovering and developing new

materials. During the 1970's, research was picked up by the nuclear industry for possible applications in new reactors or as part of the matrix fuel designs [17]. Silicon carbide (SiC) has been the standard ceramic used for many reactor fuel applications; however, the thermal dissociation and chemical attack by the fission products of palladium causes the SiC to lose some of the mechanical integrity at 1700°C and above, which limits reactor advancements [17]. The current high-temperature gas-cooled reactor (HTGR) uses Triso-coated fuel particles, which are made up of several layers surrounding an oxide or oxycarbide fuel [17]. The layers consist of porous carbon, pyrolytic carbon, SiC and another pyrolytic carbon layer [17]. The SiC layer loses strength and degrades at elevated operating temperatures (1700°C), which leads to release of fission products [17]. Recent research for the very-high-temperature reactor (VHTR) has focused on materials such as ZrC because of its high melting temperature (3445°C), high stability in aggressive chemical and radiation environments, high stiffness (392 GPa), and high hardness (20 GPa) [16,17].

Few references are available for studies of the properties of ZrC and some of the existing studies have contradictory results. For example, the melting temperature varies among reports. The phase diagram produced by Rudy [19], (Figure 2-4) shows the melting temperature dependence on carbon content in the ZrC phase with a peak melting temperature at 3445°C. Another commonly reported melting temperature is 3540°C [8,20,21].

Mechanical properties, such as strength and fracture toughness, for bulk ZrC have been described in only a few published reports. Landwehr produced bulk ZrC by hot pressing and reported a strength of 320 MPa and a hardness of 20 GPa [16]. Strength

values approaching 400 MPa and hardness values up to 25 GPa have been reported[22]. The strength of ZrC is thus comparable to other technical ceramics such as  $\text{Al}_2\text{O}_3$  [23], but is roughly half of monolithic W at room temperature.

Different methods have been used to produce bulk ZrC, including hot pressing, reactive sintering, spark plasma sintering and pressureless sintering [18,22,24]. Producing ZrC by hot pressing at 2200°C and 30 MPa resulted in 98% relative density [16]. Reactive sintering typically is where  $\text{ZrO}_2$  or Zr is reacted with graphitic carbon to form ZrC [25,26]. Often the reaction process is during, or prior to, hot pressing to form a dense compact. Other processing methods are available to produce thin films or small components. Methods such as chemical vapor deposition (CVD), physical vapor deposition (PVD) or pulsed laser deposition are used to produce ZrC thin films for coating materials like titanium and silicon.

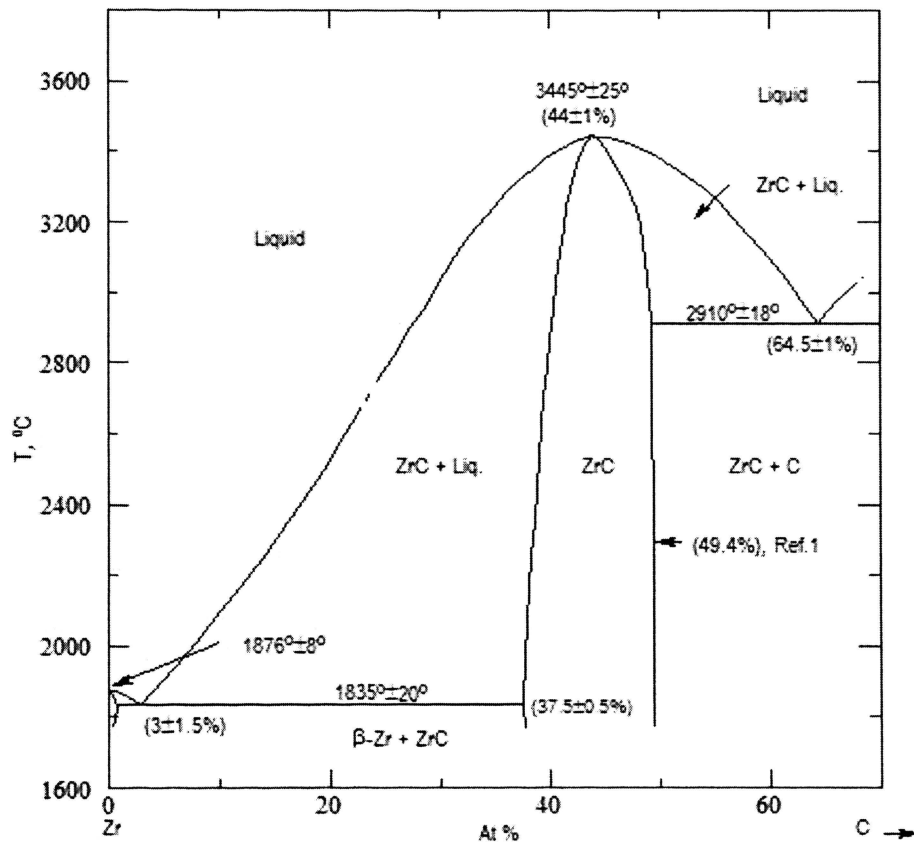


Figure 2-4: Zr-C phase diagram [27].

### 2.3. ZIRCONIUM CARBIDE – TUNGSTEN CERMETS

Composite materials can have different architectures and can be particle or fiber reinforced [28]. The phase boundaries are often weak points in composites, which can serve as failure origins. For reinforcement of a brittle phase by a ductile one, the boundary between the phases needs to be able to transfer load from the matrix to the reinforcement, so the adhesion has to be optimized in order to obtain the best performance [29]. Fibers are often laid out in layers such that the fibers are evenly distributed and in a predetermined direction to maximize performance in a particular

application. Random fiber orientation and particle reinforcement are best suited for applications where isotropic properties are desired [30]. Particle-reinforced cermets can be fabricated by powder metallurgy; however, predicting the properties is a complicated process and often only results in an estimated performance level [30].

Recent research has investigated structures in which both phases are interconnected throughout a composite material; this is referred to as an interpenetrating phase composite [31,32]. One benefit of an interpenetrating phase structure is that both materials are continuous through the component and allow for transport properties, such as electric conductivity or thermal conductivity, in one phase while the other may provide the structure and strength of the material [31]. For example, a cermet with an interpenetrating structure may have the strength and stiffness of a ceramic combined with the electrical conductivity of a metal.

One method by which interpenetrating phase composite formation can be achieved is displacive compensation of porosity (DCP). Some of the compositions that have been formed by DCP include MgO/Mg-Al, MgAl<sub>2</sub>O<sub>4</sub>/Fe-Ni-Al, and ZrC/W [21,33,34]. The DCP process uses porous preforms that are infiltrated with the second phase that can react with the preform to produce the desired composite phases. ZrC/W rocket nozzle liners have been formed by this process and tested in a Pi-K rocket motor test and showed resistance to thermal shock and erosion [21]. DCP allows for near net-shape formation without extensive finishing as well as lower production temperatures [21]. However, DCP often requires a lower melting phase such that it may be infiltrated as a liquid. In the case of ZrC/W, the WC was WC infiltrated with Zr<sub>2</sub>Cu, which was reacted to form ZrC/W. However, some Cu was still present in the final composite [21].

Another processing method, for interpenetrating phase composites, is powder processing so that both phases are interconnected through the microstructure. Work with Ni-Al<sub>2</sub>O<sub>3</sub> has shown that at depending on the starting powder size and content interpenetrating phases can be formed by powder processing techniques [21].

In an interpenetrating microstructure composite, the volume fraction for percolation has wide compositional limits, allowing essentially any volume percent of either phase, in a two phase material, to be used. The increase in the secondary material allows for a larger range of possible mechanical, chemical, and physical property combinations.

ZrC-W cermets have been prepared by various processing methods and with different ratios of ZrC to W. S.C. Zhang has developed an innovative in situ reaction sintering process that produced ZrC-W cermets by reacting ZrO<sub>2</sub> with WC to produce cermets containing 35 vol% ZrC [8]. Dickerson studied displacive compensation of porosity as a method to make near net-shaped ZrC-W components containing 50 vol% ZrC with 19 vol% W and 31 vol% WC [21]. Taiquan Zhang prepared 30 vol% ZrC cermets by hot pressing the constituent phases. The T. Zhang study also reported the compressive behavior at elevated temperatures, temperature gradient effects, clustering effects of the ZrC phase, and heat treatment effects [7,14,35,36,37] Finally, Song tested hot-pressed ZrC-W cermets from 0 vol% to 40 vol% ZrC additions; his work focused on elevated temperature mechanical properties and ablation resistance for ZrC/W cermets with 30 vol% ZrC additions [6,38,39,40,41]. Any processing methods can be used to produce the full range of ZrC additions in W. The method that is the most limited is the DCP due to the necessity of using a WC preform, and the exact range of possible ZrC

additions is unknown. Although not all authors reported properties for their materials, the mechanical properties of the materials produced by S. C. Zhang and G. M. Song are summarized in Table 2-1.

Table 2-1: Mechanical properties tested at room temperature for ZrC-W cermets.

Processing Method	Vol. % ZrC	Strength (MPa)	Elastic Modulus (GPa)	Hardness (GPa)	Fracture Toughness (MPa m <sup>1/2</sup> )
Hot Pressing [6]	30	705	383	5.77	9.23
In Situ Reaction Sintering [8]	35	402	274	6.2	8.3

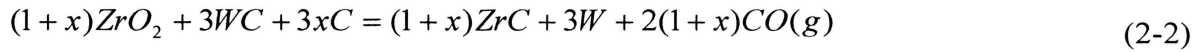
S. C. Zhang used in situ reaction sintering to make ZrC/W cermets containing 35 vol% ZrC (Reaction 2-1). In situ reaction sintering resulted in a specimen with 95% relative density. Compared to the hot pressed 30 vol% ZrC/W cermet prepared by Song, reaction sintering resulted in lower strength, toughness, and elastic modulus. The decrease in the strength, elastic modulus and fracture toughness can be attributed to the increase in porosity. The higher hardness was because of the increase in volume percent of ZrC (20 GPa) [16] compared to W (3.4 GPa) [6].



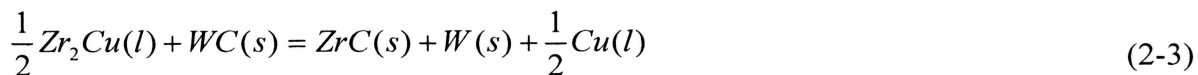
In addition to cermets containing 35 vol% ZrC, S. C. Zhang also produced cermets containing 50 vol% ZrC (Reaction 2-2) by in situ reaction sintering of ZrO<sub>2</sub> and



WC with extra carbon and  $ZrO_2$ . A relative density of 98% was achieved. However, no mechanical testing was performed on this composition [8].



Dickerson's research used DCP as the processing method for ZrC/W cermets. WC porous preforms were infiltrated with  $Zr_2Cu$  and reacted by Reaction 2-3. Interestingly, some of the Cu was forced out of the composite as a liquid during the densification process. While this material was not tested for mechanical properties, a near net shaped rocket nozzle was formed and tested in a Pi-K rocket test. The material survived the thermal shock and erosive conditions [21].



## 2.4. PROCESSING METHODS

The research in this thesis employs two processing methods to produce ZrC/W cermets: hot pressing and in situ reaction sintering. The volume ratio of 35 vol% ZrC showed potential control of the microstructure by changing sintering temperature during the in situ reaction sintering process. Furthermore, the ratio of the materials was altered to show potential for control of mechanical properties by altering the volume ratio of ZrC to W. The compositions tested contained 35 vol%, 50 vol% and 65 vol% ZrC with the remaining amount as tungsten. Each composition was prepared using both processing methods.

**2.4.1. Conventional Hot Pressing.** Conventional hot pressing is a standard production method for high temperature materials that are difficult to densify by conventional pressureless sintering. The addition of pressure often allows for reducing the temperature needed to densify materials.

The processing parameters used by Song, for hot pressing 30 vol% ZrC, ZrC-W cermets were 2000°C and 20MPa for one hour [6]. Others have used higher temperature and pressure to densify 30 vol% ZrC ZrC-W cermets on the order of 2200°C and 25 MPa for 2 hours. Lower sintering temperatures can be used with an increase in pressure. The temperature and pressure are also determined based on the amount of ZrC in the composite. The present study shows that increasing the ZrC content allows a decrease in sintering temperature. Specimens with 35 vol% ZrC were 98% of their relative density when hot pressed at 1900°C and 32 MPa while the specimen with 65 vol% ZrC reached nearly 100% relative density at 1800°C and 32 MPa.

Hot pressing in this form uses a graphite die with a typical cross-section that is round or rectangular. The removable top and bottom rams are push from the top and bottom compressing the powder compact. For this study, the limit used for safe application of the load to the compacted die was 32 MPa. The applied pressure results in better compaction of the powders when heated. In addition the pressure reduces grain growth while achieving higher density. However, hot pressing is not typically attractive for commercial applications process because the cost of dies and limited shapes increase the cost of producing parts. Hot pressing is only used when the materials cannot be densified by other sintering methods.

**2.4.2. In Situ Reaction Sintering.** In situ reaction sintering is a novel process that combines synthesis of the desired phases with densification into one process. For this process, no external pressure is applied to the specimens during the sintering cycle and it is, therefore, considered to be a pressureless process. In general, in situ reaction sintering can be considered a two step process consisting of separate reaction and densification steps. For the reaction under consideration in the present study, the first step in the heating cycle is for the reaction, which occurs at a lower temperature than densification. The furnace is held at the lower temperature(s) for the reaction to reach completion. For  $ZrO_2$  and WC, the reaction typically occurs around  $1250^\circ C$  and takes about an hour to go to completion under vacuum. However, the time and temperature of the reaction are dependent on the size in volume of the specimens. Those with larger volumes require longer reaction times based on the need to remove gaseous reaction products without causing a buildup of pressure within the specimen. After the reaction has gone to completion, the furnace can be increased to a temperature that allows for densification. The sintering temperature in this process is typically higher than the temperature required to produce a dense cermet by hot pressing. After reaction and densification, the system is then cooled and the part is ready for characterization and testing. This process allows for the production of more complex shapes than hot pressing, which is generally not limited to specimens with circular or rectangular cross sections. The parts can be any shape capable of being formed by powder processing and/or green machining.

## 2.5. REFERENCES

- [1] Askeland, Donald R. Pradeep P. Phulé, *Essentials of Materials Science and Engineering*, Thomson, Ontario, Canada, 2004.
- [2] S. W. H. Yih C. Wang, *Tungsten: Sources, Metallurgy, Properties, and Applications*, Plenum Press, New York, 1979.
- [3] A. G. Metcalfe, N. B. Elsner, E. Wuchina, M. Opeka, "Oxidation above 3300°C of refractory materials in an aluminized flame," *Proceedings—Electrochemical Society 2003-16 (High Temperature Corrosion and Materials Chemistry IV)*, Paris, France, 2003 pp. 420-30.
- [4] Tinklepaugh, J.R. W. B. Crandell, *Cermets*, Reinhold Publishing Corporation, New York, 1960.
- [5] C. R. Manning, JR., R. F. Stoops, "High-Temperature Cermets: I, Compatibility," *J. Am. Ceram. Soc.* 51[8] (1968) 411-414.
- [6] G. M. Song, Y. J. Wang, and Y. Zhou, "The Mechanical and Thermophysical Properties of ZrC/W Composites at Elevated Temperature," *Mater. Sci. Eng. A* 334 (2002) 223-32.
- [7] T. Zhang, Y.J. Wang, Y. Zhou, G. M. Song, "Effect of heat treatment on microstructure and mechanical properties of ZrC particles reinforced tungsten-matrix composites," *Mater. Sci. Eng. A* 512 (2009) 19-25.
- [8] S. C. Zhang, G. E. Hilmas, W. G. Fahrenholtz. "Zirconium Carbide-Tungsten Cermets Prepared by In Situ Reaction Sintering," *J. Am. Ceram. Soc.* 90[6] (2007) 1930-33.
- [9] S. C. Zhang, G. E. Hilmas, W. G. Fahrenholtz, US patent 7 648 675, 19 January 2010.
- [10] J. A. Vaccari, G. S. Brady, H. R. Clauser, *Materials Handbook* (15<sup>th</sup> Ed.). McGraw-Hill, New York, 2002.
- [11] M. Faleschini, H. Kreuzer, D. Kiener, R. Pippan, "Fracture toughness investigations of tungsten alloys and SPD tungsten alloys." *J. Nucl. Mater.* 367-370 (2007) 800-805.
- [12] E. Lassner, W. D. Schubert. *Tungsten: Properties, Chemistry, Technology of the Element, Alloys, and Chemical Compounds*, Plenum Publishers, New York, 1999.
- [13] G. W. King, H. G. Sell, "The effect of thoria on the elevated-temperature tensile properties of recrystallized high-purity tungsten." *Trans. Am. Inst. of Min., Metall. Pet. Eng.* 233[6] (1965) 1104-13.

- [14] T. Zhang, Y. J. Wang, Y. Zhou, T. Q. Lei, G. M. Song, "Compressive deformation behavior of 30 vol.% ZrC<sub>p</sub>/W composite at temperatures of 1300-1600°C," *Mater. Sci. Eng. A* 474 (2008) 382-389.
- [15] K. Upadhyaya, J. M. Yang, W. P. Hoffman, "Materials for ultrahigh temperature structural applications," *Am. Ceram. Bull.*, December 1997.
- [16] S. E. Landwehr, G. E. Hilmas, W. G. Fahrenholtz, I. G. Talmy, S. G. DiPietro, "Microstructure and mechanical characterization of ZrC-Mo cermets produced by hot isostatic pressing," *Mater. Sci. Eng. A* 497 (2008) 79-86.
- [17] S. Ueta, J. Aihara, A. Yasuda, H. Ishibashi, T. Takayama, K. Sawa, "Fabrication of uniform ZrC coating layer for the coated fuel particle of the very high temperature reactor," *J. Nucl. Mater.* 376 (2008) 146-151.
- [18] G. Vasudevamurthy, T. W. Knight, E. Roberts, T. M. Adams, "Laboratory production of zirconium carbide compacts for use in inert matrix fuels," *J. Nucl. Mater.* 374 (2008) 241-247.
- [19] E. Rudy, *Compendium of Phase Diagram Data*, Air Force Materials Laboratory Metals and Ceramics Division, Wright-Patterson AFB, OH, 1969, pp. 162.
- [20] Y. Yang, C. A. Dickerson, H. Swoboda, B. Miller, T. R. Allen, "Microstructure and mechanical properties of proton irradiated zirconium carbide," *J. Nucl. Mater.* 378 (2008) 341-348.
- [21] M. B. Dickerson, P. J. Wurm, J. R. Schorr, et. al., "Near net-shape, ultra-high melting, recession-resistant ZrC/W-based rocket nozzle liners via the displacive compensation of porosity (DCP) method," *J. Mat. Sci.* 39 (2004) 6005-6015.
- [22] D. Sciti, S. Guicciardi, M. Nygren, "Spark plasma sintering and mechanical behavior of ZrC-based composites," *Scr. Mater.* 59 (2008) 638-641.
- [23] M. Miyayama, K. Koumoto, H. Yanagida, in: S.J. Schneider, Jr. (Eds.), "Engineering Properties of Single Oxides," *Engineered Materials Handbook Volume 4: Glasses and Ceramics*, ASM International, Materials Park, OH, 1991, pp. 748-757.
- [24] W. Han, Z. Wang, "Fabrication and oxidation behavior of a reaction derived graphite-ZrC composite for ultrahigh temperature applications," *Mater. Lett.* 63 (2009) 2175-2177.
- [25] G. Vasudevamurthy, T.W. Knight, E. Roberts, T. M. Adams, "Laboratory production of zirconium carbide compacts for use in inert matrix fuels," *J. Nucl. Mater.* 374 (2008) 241-47.

- [26] B. D. Pollock, "The Vaporization Behavior and Thermodynamic Stability of Zirconium Carbide at High Temperature," *The J. Phys. Chem.* 65 (5) (1961) 731–735
- [27] E. Rudy, D. P. Harmon, C. E. Brukl, *ACerS – NIST Phase Equilibria Diagrams Version 3.0.1*, The American Ceramic Society Westerville, Ohio, 2004.
- [28] B. D. Agarwal, L. J. Broutman, K. Chandrashekhara, *Analysis and Performance of Fiber Composites*, John Wiley and Sons Inc. Hoboken, New Jersey, 2006.
- [29] L. T. Drzal, "Interfaces and Interphases" *ASM Handbook Vol. 21 Composites* p. 169.
- [30] D. B. Miracle, S. L. Donaldson, "Introduction to Composites," *ASM Handbook Vol. 21 Composites* p. 6.
- [31] D. R. Clarke, "Interpenetrating Phase Composites," *J. Am. Ceram. Soc.* 75[4] (1992) 739-759.
- [32] A. Mattern, B. Huchler, D. Staudenecker, R. Oberacker, A. Nagel, M. J. Hoffmann, "Preparation of interpenetrating ceramic-metal composites," *J. Euro. Ceram. Soc.* 24 (2004) 3399-3408.
- [33] P. Kumar, K. H. Sandhage, "The displacive compensation of porosity (DCP) method for fabricating dense, shaped, high-ceramic-bearing bodies at modest temperatures," *J. Mater. Sci.* 34 (1999) 5757-5769.
- [34] K. A. Rodgers, P. Kumar, R. Citak, K. H. Sandhage, "Dense, shaped ceramic/metal composites at  $\leq 1000^\circ\text{C}$  by the displacive compensation of porosity (DCP) method," *J. Am. Ceram. Soc.* 82[3] (1999) 757-60.
- [35] T. Zhang, Y. J. Wang, Y. Zhou, T. Q. Lei, G. M. Song, "Elevated temperature compressive failure behavior of a 30 vol.%  $\text{ZrC}_p/\text{W}$  composite," *Int. J. Refract. Met. Hard Mater.* 25 (2007) 445-450.
- [36] T. Zhang, Y. J. Wang, Y. Zhou, G. M. Song, "Effect of temperature gradient in the disk during sintering on microstructure and mechanical properties of  $\text{ZrC}_p/\text{W}$  composite," *Int. J. Refract. Met. Hard Mater.* 27 (2009) 126-129.
- [37] T. Zhang, Y. J. Wang, Y. Zhou, G. M. Song, "Effect of particle clustering on the effective modulus of  $\text{ZrC}/\text{W}$  composites," *Int. J. Refract. Met. Hard Mater.* 27 (2009) 14-19.
- [38] G. M. Song, Y. J. Wang, Y. Zhou, "The Influence of  $\text{ZrC}$  particle content on the mechanical properties of tungsten matrix composites," *Nonferr. Met. (Youse Jinshu)* 53[1] (2001) 47-51.

[39] G. M. Song, Y. Zhou, Y. J. Wang, T. C. Lei, "Elevated temperature strength of a 20 vol% ZrC<sub>p</sub>/W composite," *J. Mater. Sci. Lett.* 17 (1998) 1739-1741.

[40] G. M. Song, Y. J. Wang, Y. Zhou, "Elevated temperature ablation resistance and thermophysical properties of tungsten matrix composites reinforced with ZrC particles," *J. Mater. Sci.* 36 (2001) 4625-4631.

[41] G. M. Song, Y. Zhou, Y. J. Wang, "Effect of carbide particles on the ablation properties of tungsten composites," *Mater. Charact.* 50 (2003) 293-303.

## PAPER

**I. MICROSTRUCTURE AND MECHANICAL PROPERTIES OF ZrC-W  
CERMETS**

Melissa M. Giles, S. C. Zhang, W.G. Fahrenholtz, G.E. Hilmas

**1.1 ABSTRACT**

The microstructure and mechanical properties of zirconium carbide-tungsten cermets prepared by two different processing methods, in situ reaction sintering and hot pressing, were compared. The ZrC-W cermets contained 35 vol% ZrC and had relative densities greater than 97%. The reaction sintered specimens were processed at two different final sintering temperatures that produced comparable relative densities, but different microstructural feature sizes. For in situ reaction sintering at 2050°C, the feature size was  $<1\mu\text{m}$ , compared to  $>2\mu\text{m}$  after processing at 2100°C. For comparison, hot pressing at 2050°C produced a relative density of  $\sim 99\%$  and a feature size of  $<1\mu\text{m}$ . Hot pressed cermets had the highest room temperature strength at  $\sim 760\text{ MPa}$ , while the cermet that was reaction sintered at 2100°C had the highest hardness at  $\sim 10\text{ GPa}$  and the highest fracture toughness at  $\sim 8\text{ MPa}\cdot\text{m}^{1/2}$ . The results demonstrated that by controlling the processing method and the sintering temperature, the properties of the resulting cermets could be tailored.

**1.2 INTRODUCTION**

Tungsten (W) is a refractory metal with a density of  $19.3\text{ g/cm}^3$ . High density is a concern for aerospace applications where reduced weight of structural materials translates



directly into increased payload or reduced fuel consumption [1]. Because W has a melting point greater than 3000°C, which is the highest melting temperature of the refractory metals, it is one of the few options for applications with a high operating temperature such as rocket nozzles, tubing in nuclear reactors, and combustion chambers [2,3,4].

While the strength of W is nearly 800 MPa at room temperature, the strength decreases rapidly as temperature increases, dropping to 60% or less of the room temperature strength when the temperature exceeds 1000°C [3,4]. In addition, W is a hard metal with a hardness of 3.4 GPa, and its high ductile to brittle transition temperature (~400°C) makes it difficult to machine at room temperature [3]. Alloying is one method that has been used improve the elevated temperature strength and increase the workability of W [4].

Alloying additions of Rhenium (Re) lower the ductile to brittle transformation temperature and increase the strength of W at elevated temperatures [2,3,4,5]. Tungsten-rhenium (W 25 wt. %Re) alloys lower the ductile brittle transition temperature to -50°C, compared to 400°C for pure tungsten, and a tensile strength of around 1400 MPa at room temperature compared to ~800 MPa for monolithic W. Adding Re increases the elevated temperature strength to ~250 MPa at 1926°C [4,5]. However, the strength of the alloy drops to ~50 MPa by 2100°C, which is the about same as pure tungsten at this temperature [4]. For ultra-high temperature applications, the property improvement due to Re additions is minimal, especially considering its cost. Re in 1998 cost \$900/kg, compared to W which cost \$8/kg [6]. Further, the goal of achieving higher strengths at temperatures around 2000°C is not likely to be reached by alloying alone.

The addition of a second phase affects the mechanical properties of tungsten [2,3,4,7]. To improve the elevated temperature mechanical properties, a material with good high temperature properties is required. Fine ceramic particles such as  $\text{La}_2\text{O}_3$ ,  $\text{ThO}_2$ ,  $\text{ZrC}$ ,  $\text{HfC}$ ,  $\text{TiC}$ , and  $\text{Ta}_2\text{C}$  have been added to W [4,8,9,10,11,12]. Carbides are generally chemically compatible with W and typically form limited solid solution. The additions of ceramic particles have demonstrated improved elevated temperature strength, but often with an accompanying decrease in room temperature strength [3,13].

Zirconium carbide is an attractive second phase for W-based cermets because of its similar melting point ( $3445^\circ\text{C}$  for  $\text{ZrC}$  compared to  $3422^\circ\text{C}$  for W) and thermal expansion coefficient ( $4.0 \times 10^{-6}/^\circ\text{C}$  for  $\text{ZrC}$  compared to  $4.5 \times 10^{-6}/^\circ\text{C}$  for W at room temperature) [14,15]. The lower density of  $\text{ZrC}$  ( $6.74 \text{ g/cm}^3$ ) is an additional benefit, especially for designs in aerospace where weight is a key design criterion [16].

Hot pressing has been used to form  $\text{ZrC}$ -W cermets in the ratio of 30 vol%  $\text{ZrC}$  to 70 vol% W [3]. The resulting composite material had a flexure strength of  $\sim 700 \text{ MPa}$  compared to  $\sim 800 \text{ MPa}$  for monolithic W [3]. The strength increased with increasing temperature to a peak of  $\sim 830 \text{ MPa}$  around  $1000^\circ\text{C}$  [3]. The addition of  $\text{ZrC}$  also improved fracture toughness at room temperature [3].

Another method of forming  $\text{ZrC}$ -W cermets is in situ reaction sintering. Zhang et al. formed cermets composed of 35 vol%  $\text{ZrC}$  and 65 vol% W by in situ reaction sintering [2]. The resulting composites had a relative density of 95% dense, a room temperature strength of  $\sim 400 \text{ MPa}$ , and a fracture toughness of  $8.3 \text{ MPa m}^{1/2}$  [2]. This composition was formed by reacting  $\text{ZrO}_2$  with WC by the following reaction.



The purpose of this paper was to compare the microstructures and room temperature mechanical properties of ZrC-W cermets prepared by two different processing methods, conventional hot pressing and in situ reaction sintering.

### 1.3 EXPERIMENTAL PROCEDURE

**1.3.1 Processing.** Commercial powders were used as the starting materials. The WC (< 1 $\mu\text{m}$ , 99% purity, Cerac Inc. Milwaukee, WI) and ZrO<sub>2</sub> (-325 mesh, >99% purity, Alfa Aesar Chemical Co., Ward Hill, MA) were batched to achieve the stoichiometric ratio shown in Reaction 1-1. The ZrO<sub>2</sub> powders were attrition milled using yttria stabilized zirconia media in ethanol for 2 hours to reduce the particle size. The average particle size (d<sub>50</sub>) measured using laser light scattering (Microtrack model S3500, Microtrac Inc.) was 0.42  $\mu\text{m}$  after attrition milling. The attrition milled ZrO<sub>2</sub> and as-received WC powders were mixed by ball milling for 48 hours in acetone with WC media to form a homogeneous mixture. In addition, 5 mg of dispersant (DISPERBYK-110, BYK-Chemie Co., Wesel, Germany) was added per square meter of estimated surface area of the powders. The surface area was calculated from the reported particle size based on the assumption of spherical particles. After mixing, powders were dried while continuously stirring on a hot plate that was less than 100°C. The dried powders were crushed with a mortar and pestle and sieved to -80 mesh. Pellets for a sintering study were pressed in a 1.3 cm (0.5 inch) diameter circular die. A rectangular steel die, 2.5 cm wide by 5.7 cm long (1 in by 2.25 in), was used to press bars for strength and

fracture toughness testing. Pellets were formed by uniaxially pressing to 3.4 MPa (500 psi) followed by cold isostatic pressing to 207 MPa (30 ksi). Pellets were then sintered at temperatures between 1900°C and 2150°C for the densification study. The furnace was heated under vacuum (~20 Pa) at 10°C per minute from room temperature to 1850°C. Isothermal holds were used at 1250°C for 1.5 hours and 1650°C for 1 hour to allow recovery of the vacuum. An additional hold was added at 1850°C to switch the furnace atmosphere to flowing argon at an over pressure of approximately 20 kPa (gauge pressure). The furnace was heated to the final sintering temperature at a rate of 20°C per minute and held for 4 hours. Specimens for mechanical testing were larger, so a slower rate of 5°C per minute was used between 1250°C and 1850°C with holds of 1 hour at 1250, 1650 and 1850°C. Specimens were heated to the final sintering temperature at 10°C per minute and held for 4 hours at 2050 or 2100°C.

For comparison to pellets produced by in situ reaction sintering, additional specimens were prepared by hot pressing commercially available ZrC (-325 mesh, >99.5% purity, Cerac Inc., Milwaukee, WI) and W (1-5 micron, >99.9% purity, Alfa Aesar Ward Hill, MA) powders. The ZrC was attrition milled with WC media to further reduce its particle size. The ZrC and W were then mixed by ball milling with WC media for 24 hours in ethanol with 1 wt% of dispersant (DISPERBYK-110, BYK-Chemie Co., Wesel, Germany). The powders were dried, crushed using a mortar and pestle, and sieved to -80 mesh. The powders were then packed in a 4.5 cm (1.75 in) diameter graphite die lined with graphoil that had been coated with boron nitride (BN) spray to minimize reaction between the powder and the die. Specimens were hot-pressed at 1900°C or 2050°C. The furnace was heated at 20°C/min under vacuum (~20 Pa) to 1650°C without

load and the temperature was held at 1650°C to allow for decomposition of surface oxides. After the hold, the furnace atmosphere was switched to flowing argon and a uniaxial load of 32 MPa was applied. The furnace temperature was increased at a rate of 20°C/min to the final densification temperature of 1900°C or 2050°C. The specimens were held at temperature for 10 min after the ram travel ceased. Total time at temperature was typically an hour. The furnace was cooled at approximately 20°C/min. The pressure was released after the furnace cooled below 1650°C.

**1.3.2 Characterization.** Archimedes' method was used to measure the bulk density of the sintered specimens. Water was used as the immersion medium. The theoretical density calculated based on the amounts of ZrC and W expected in the final product based on the stoichiometry of Reaction 1-1. The composites were estimated to contain 35 vol% ZrC and 65 vol% W, which results in a theoretical density of 14.9 g/cm<sup>3</sup> (~20% less than pure W). The relative density was calculated by dividing the measured bulk density by the estimated theoretical density.

X-ray diffraction (XRD;  $\theta$ - $\theta$  type XDS200 X-ray diffractometer XDS 2000, Scintag Inc., Cupertino, CA) was performed on powders produced by grinding specimens produced by in situ reaction sintering or hot pressing. The scan was performed on a packed powder mount using Cu-K $\alpha$  radiation in step mode using a step size of 0.03 deg. and a count time of 2 seconds at each step.

Microstructures were analyzed using scanning electron microscopy (SEM; S570 or S4700, Hitachi, Tokyo, Japan). The top of the pellets were ground flat using a 125  $\mu$ m grit polishing pad. The ground surfaces were polished using diamond slurries down to 0.25  $\mu$ m for microstructure analysis. Measurements of porosity and feature size were

performed using image analysis software (Image J, National Institutes of Health, Washington, DC). The feature size was measured by taking the average of the diameter of the features.

**1.3.3 Mechanical Testing.** The specimens for flexure strength testing were prepared according to ASTM Standard C1161-02c for size A bars (25 mm by 2.0 mm by 1.5 mm), the edges were chamfered, and the tensile surfaces were polished using a diamond slurry to 1 $\mu$ m. Strengths were tested in four point bending using a screw driven load frame (Model 5881, Instron, Norwood, MA) and a fully articulated four point bend fixture. Hardness was measured using a minimum of 10 Vickers' indents using a 4.9 N load and a dwell of 10 seconds (Duramin 5, Struers, Westlake, OH) following ASTM Standard C1327-03.

Fracture toughness was measured using the chevron notch method described in ASTM Standard C 1421-01b. Rectangular bars were ground to 3 mm by 4 mm with a minimum length of 50 mm. All side surfaces were surface ground using a 600 grit wheel removing 2.5  $\mu$ m (0.0001 inches) per pass. The chevron notch was cut making a pass on opposite sides of the bar, with the cut ending on the bottom side of the bar. The bar was positioned at a 26° angle to achieve the necessary dimensions. A 320 grit diamond wheel was used to make the cut. The test was run using the same screw driven load frame as the strength test, but at a rate of 0.005mm/sec using a fully articulated fixture. After testing, specimens were examined using optical microscopy to make sure the notch was within the tolerances allowed by the standard.

## 1.4 RESULTS AND DISCUSSION

Using the in situ reaction sintering process described by Reaction 1-1, stoichiometric mixtures of  $\text{ZrO}_2$  and WC (1:3 molar ratio) were converted to fully dense composites containing ZrC and W. Based on experiments in which pellets were run through part of the processing cycle, densification occurred after the materials had reacted. The reaction process resulted in a calculated volume decrease of approximately ~26% based on the stoichiometry of Reaction 1-1. The volume change calculation assumed pure reactants and products along with theoretical densities of  $5.9 \text{ g/cm}^3$  for  $\text{ZrO}_2$ ,  $15.6 \text{ g/cm}^3$  for WC,  $6.7 \text{ g/cm}^3$  for ZrC, and  $19.3 \text{ g/cm}^3$  for W. The measured volume change from the pressed pellet to the sintered pellet was ~28%. Considering that the volume of solids in the pellet decreased due to reaction, and the pellet also shrank further to eliminate porosity present in the green state, the effective volume change during sintering was ~54% to account for the shrinkage necessary to eliminate porosity in the green body plus overcome the volume change due to reaction.

Despite the large overall volume change, pellets underwent the combined reaction and densification processes with no cracking or warping. Figure 1-1 shows pellets prior to and after in situ reaction sintering. The specimen on the right was formed by uniaxial pressing (32 MPa) and isostatic pressing (207 MPa) and had a green density of ~63%. The specimen on the left was sintered at  $2100^\circ\text{C}$  and had a relative density of ~97%.

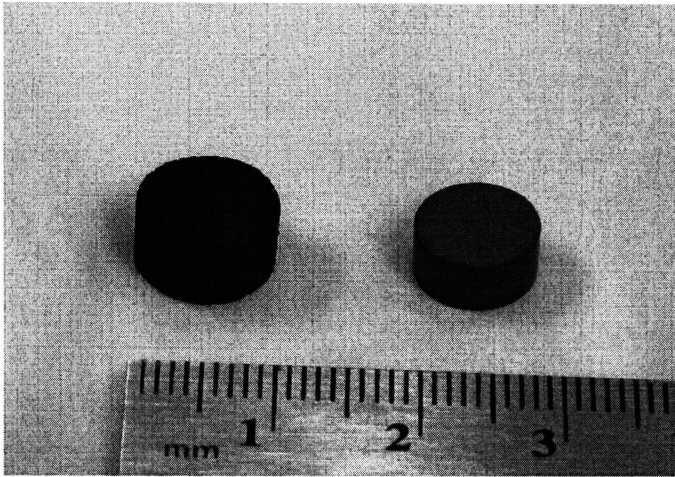


Figure 1-1: Pellets before and after in situ reaction sintering. Note that the ruler is marked in mm.

The products of Reaction 1-1 should consist of 35 vol% ZrC and 65 vol% W. Analysis of reacted specimens by XRD (Figure 1-2) showed that WC was the most prominent phase in the pattern for the unreacted specimen. For the reacted specimens, W was the most prominent phase. The W-containing phases had the highest relative intensities because of its relatively high scattering efficiency of W compounds compared to  $ZrO_2$  or ZrC. The XRD patterns showed that the reaction led to the formation of ZrC and W at all of the temperatures that were examined.



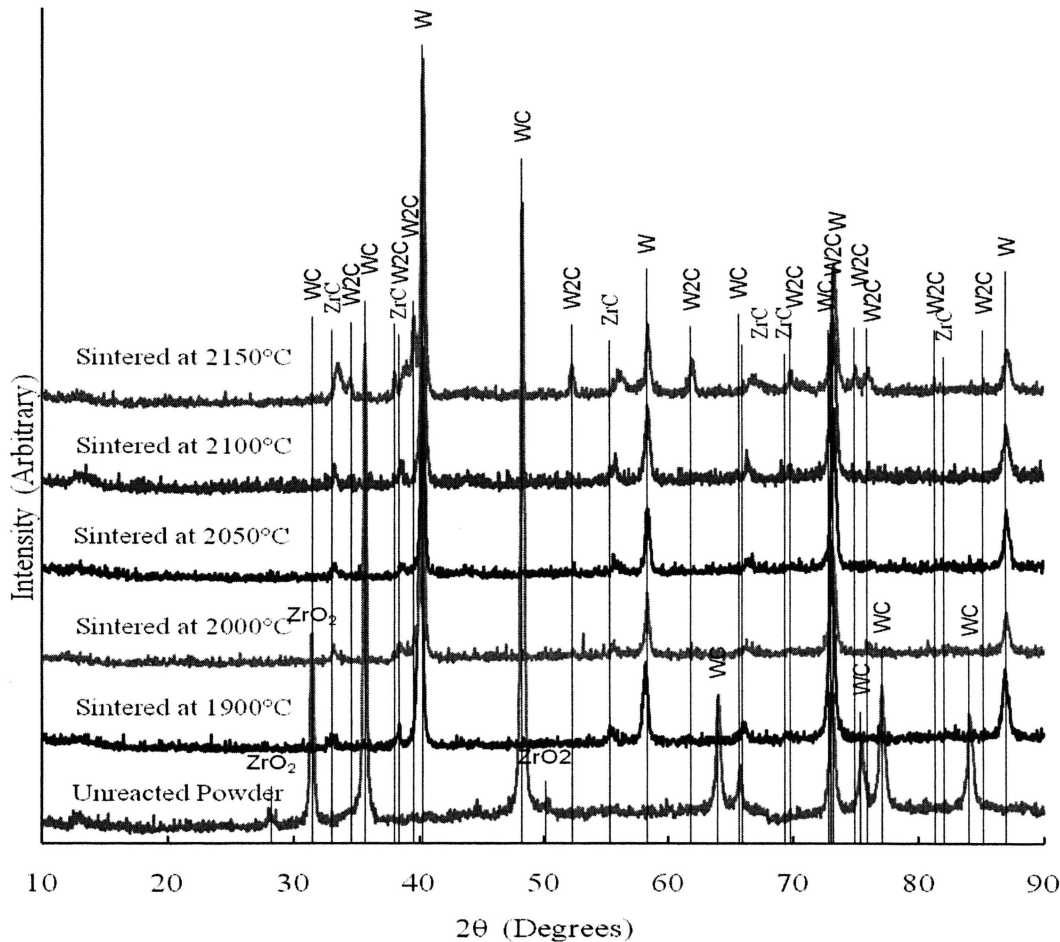


Figure 1-2: XRD patterns for the unreacted starting powders and materials that were reaction sintered at various temperatures.

Analysis of the XRD patterns revealed that the peaks for ZrC were shifted to higher angles than reported in the catalog (JCPDS card 35-0784 for ZrC). The peak shifts were quantified and used to calculate the corresponding lattice parameter using Rietveld analysis. The lattice parameter for nominally pure ZrC (rocksalt crystal structure) reported on JCPDS card 35-0784 was 4.693 Å. Substitution of W into the ZrC lattice is expected to shift the measured lattice parameters to smaller values due to the smaller covalent radius of W (1.38 Å) compared to Zr (1.57 Å). The measured lattice parameters

for ZrC after processing at all reaction sintering temperatures, as well as 2050°C for the hot pressed specimen, are summarized in Table 1-1. The solubility of W in ZrC is reported to be ~7 mol% for arc melted ZrC and W [17]. The amount of solid solution formation during the sintering process was on the order of 1.5 to 5 mol% assuming a linear relationship between the amount of W and the lattice parameter of ZrC.

Table 1-1: Lattice parameter measurements as determined from XRD analysis along with the calculated amounts W in solid solution.

Sintering Temperature	Lattice parameter ( )	W in ss (mol%)
1900°C	4.67	2.7
2000°C	4.67	2.5
2050°C	4.62	8.1
2100°C	4.63	6.8
2150°C	4.62	7.6
H.P. 2050°	4.64	5.6

\*Values of W solid solution are  $\pm 1$  mol%.

Based on XRD analysis, sintering at the highest temperature, 2150°C, resulted in the formation of a third phase,  $W_2C$ , in addition to ZrC and W. The  $W_2C$  formation may be the result of the formation of solid solutions. Zhang [18], concluded that the formation of  $W_2C$  occurred when the (Zr, W)C solid solution became supersaturated with W, which resulted in the precipitation of  $W_2C$  as the specimen cooled from the processing temperature to room temperature.

Two other possible causes of the formation of  $W_2C$  are pick up of C from the furnace or WC from milling. The additional carbon could react with W formed by Reaction 1-1 to form  $W_2C$ . Analysis of the phase diagram (Figure 1-3) [17] shows only a

narrow stability region for ZrC and W, which is labeled “ $\beta+\delta$ ”. The addition of C or WC would shift the overall composition into the three phase field that consists of ZrC, W and  $W_2C$ , which is labeled “ $\gamma+\beta+\delta$ ”.

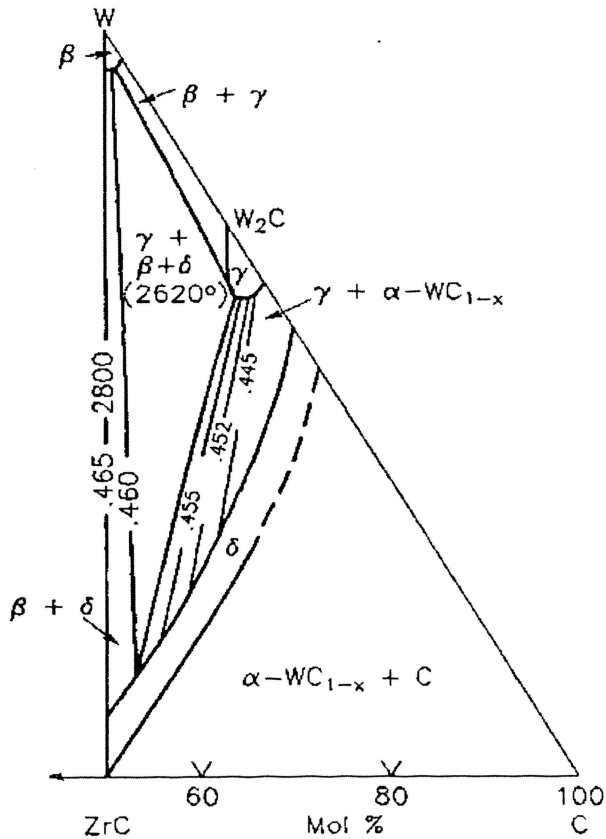


Figure 1-3: ZrC-W phase diagram [17].

Analysis of the hot pressed material using XRD revealed that the two phases present after sintering were ZrC and W. (Figure 1-4). The hot pressed samples had a similar shift in the position of the ZrC peaks due to the formation of the solid solution with W. The estimated W content in ZrC was 5.6 mol% for the hot pressed material.

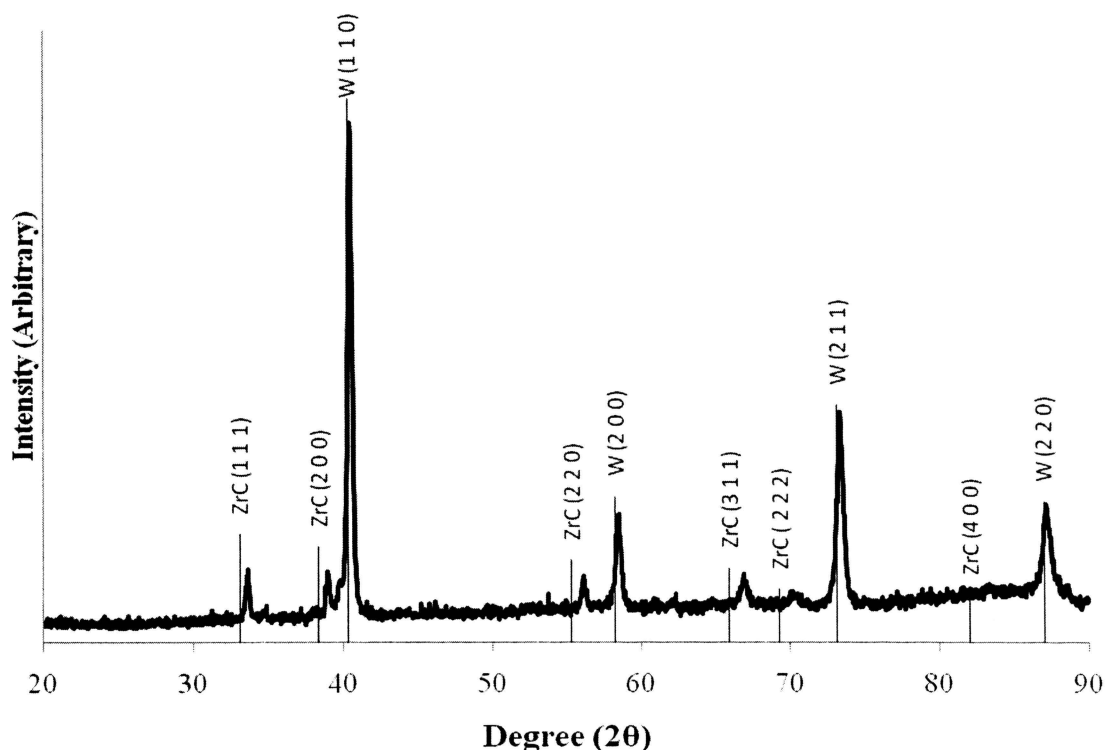


Figure 1-4: XRD spectra of the materials that were hot-pressed at 2050°C and 32MPa.

The relative density of reaction sintered ZrC-W cermets increased with increasing densification temperature up to ~2050°C (Figure 1-5). After sintering at 1900°C, the relative density was 84% and increased to 92% after sintering at 2000°C. The density peaked at 98% after sintering at 2050°C and decreased to ~97% after sintering at 2100°C. Sintering at 2150°C resulted in a further decrease in the relative density to 96%. The decrease in density is discussed in more detail below in the section discussing the microstructure. Based on similar relative density values, sintering temperatures 2050°C and 2100°C were selected for preparation of specimens for studying mechanical properties.

To further evaluate the effect of microstructure on the properties of ZrC-W cermets, additional specimens were prepared by hot pressing ZrC and W powders at 1900°C and 2050°C. The relative densities were 98% and 99% of their theoretical values. The specimens used for property measurements were hot pressed at 2050°C because this temperature produced a higher density and was closer to the processing temperatures of the reaction sintered materials.

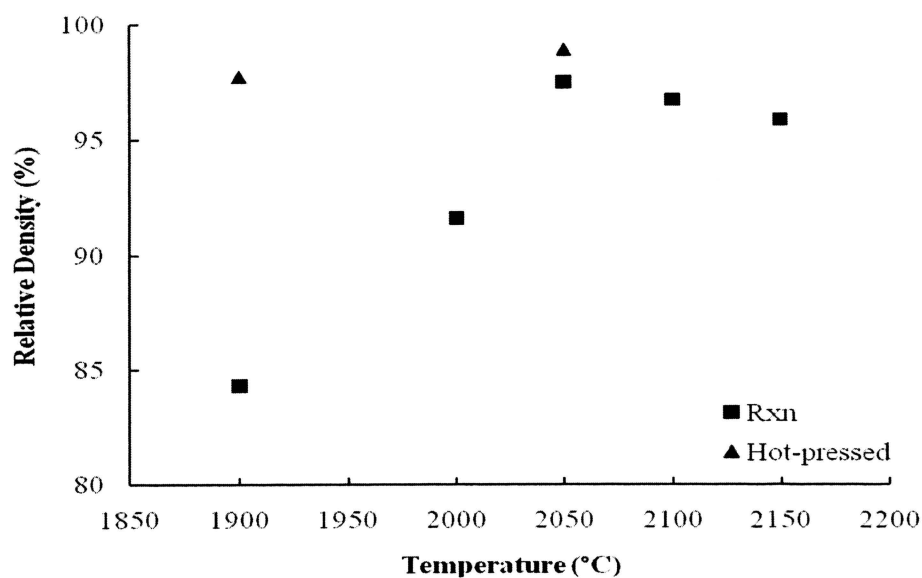


Figure 1-5: Relative density as a function of processing temperature for ZrC-W cermets prepared by in situ reaction sintering (closed squares) and conventional hot pressing (closed triangles).

SEM micrographs (Figure 1-6) show the microstructures of the in situ reaction sintered materials as a function of the final sintering temperature. The darker phase is ZrC while the lighter phase is W. After sintering at 1900°C or 2000°C, some porosity was visible. The pores were around the same size or slightly larger (~1-2  $\mu\text{m}$ ) than the

features in the two phases. At the sintering temperature of 2050°C the pores were smaller (typically  $< 1 \mu\text{m}$ ) and appeared to be isolated within the ZrC phase. For sintering temperatures 2100°C and 2150°C the porosity was contained almost completely in the ZrC phase and was  $< 1 \mu\text{m}$  in size. In addition, a greater volume fraction of porosity was observed in the micrographs,  $\sim 3 \text{ vol}\%$  for 2100°C and  $5 \text{ vol}\%$  for 2150°C. The amounts of porosity estimated from the micrographs using image analysis were close to the amounts predicted from the calculated Archimedes' densities, which were  $\sim 3\%$  and  $\sim 4\%$  respectively.

The SEM micrographs also revealed that significant growth in the size of the microstructural features occurred between 2050°C and 2100°C. The average feature size, measured using image analysis software, after sintering at 2050°C was  $0.7 \pm 0.3 \mu\text{m}$  compared to  $2.3 \pm 0.6 \mu\text{m}$  after sintering at 2100°C. This observation, that the microstructure became coarser while the relative density did not change, indicates that the process offers the potential for controlling the microstructure and, therefore, the properties, of the resulting cermets by varying the processing conditions.

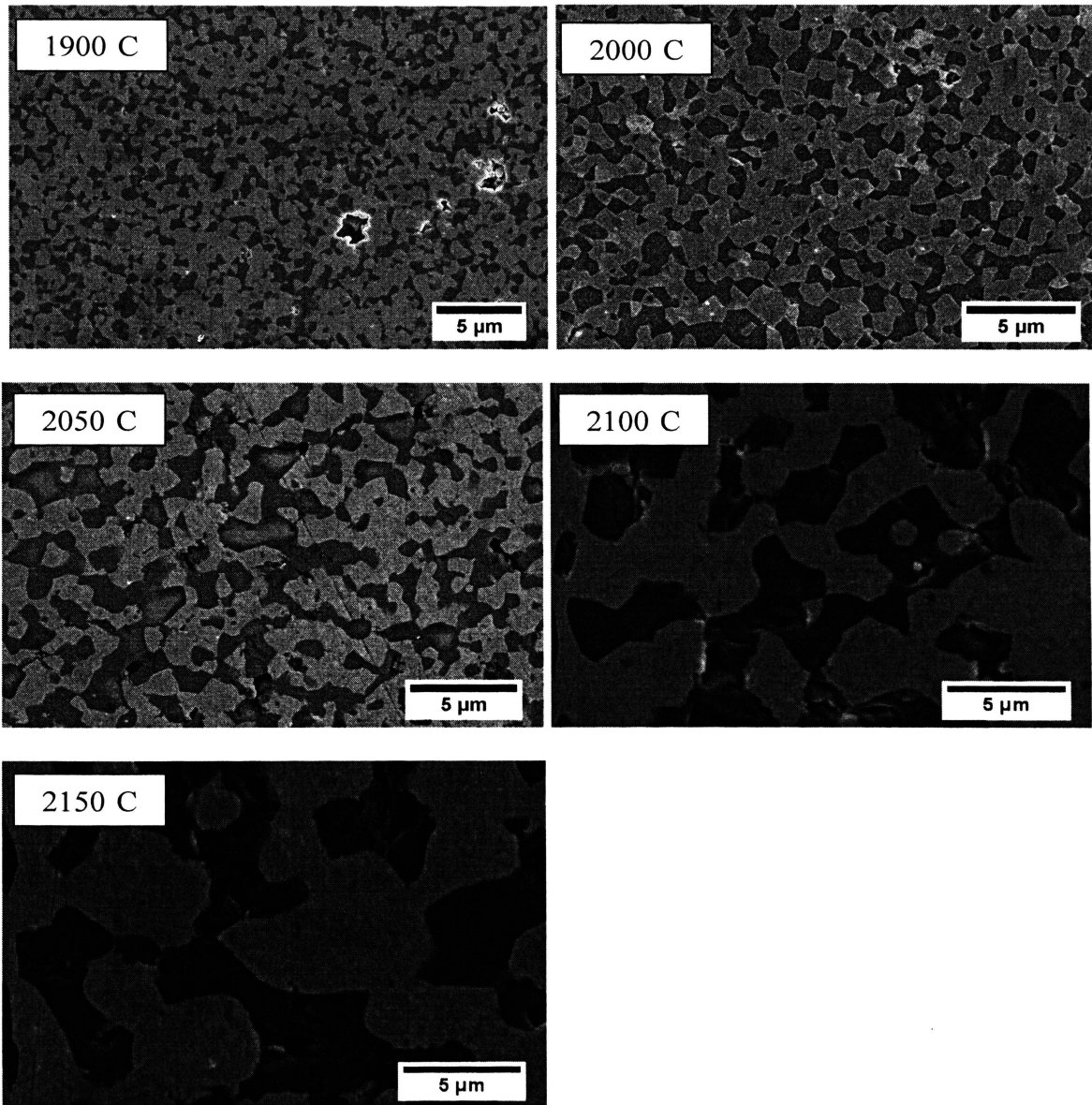


Figure 1-6: SEM images of the polished surfaces of ZrC-W cermets produced by in situ reaction sintering at different temperatures. The darker phase is ZrC, and the lighter is W.

In addition to further coarsening of the microstructure, densification at 2150°C led to an increase in the amount of porosity observed in the ZrC phase. A third phase also appeared in the XRD patterns at 2150°C, although it was not directly observed during microstructural analysis most likely due to  $W_2C$  having similar compositional contrast to

W when compared to ZrC. Analysis of XRD patterns confirmed that processing at 2150°C led to the formation of a small amount of W<sub>2</sub>C. Table 1-2 shows the amounts of each phase estimated from image analysis. The amounts of ZrC and W are consistent with what is predicted using the stoichiometric reaction for the reacted samples, which is ~35 vol% ZrC and 65 vol% W.

Table 1-2: Compositions predicted by analysis of SEM micrographs and the amount of porosity.

°C			
°C			
°C 32MPa			

Microstructural analysis of the cermet produced by hot pressing (Figure 1-7) showed features that were similar to those observed in the reaction sintered materials. The key difference was an apparent increase in clustering of the ZrC phase. The average feature size, disregarding the agglomerates, was  $0.8 \pm 0.2 \mu\text{m}$ , which was about the same as the in situ reaction material produced at 2050°C. As with the reaction sintered material, the porosity was mainly located in the ZrC phase. The amount of porosity estimated by image analysis of the micrograph was ~2 vol% which was greater than the 1 vol % porosity predicted based on Archimedes' density measurements.



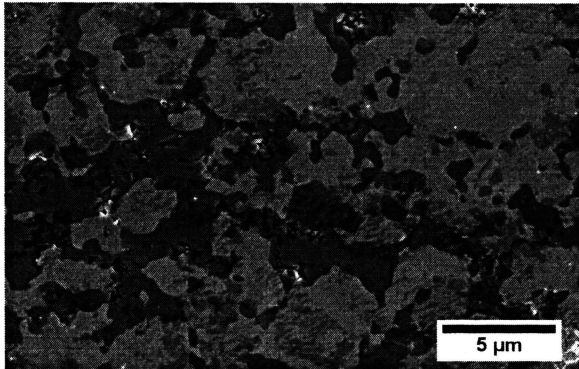


Figure 1-7: SEM micrograph of a ground and polished surface of 35 vol% ZrC, 65 vol% W cermet produced by hot pressing. The darker phase is ZrC and the lighter phase is W.

Mechanical properties were tested on ZrC-W cermets that were sintered at 2050°C and 2100°C. For comparison, properties were also tested for a ZrC-W cermet containing 35 vol% ZrC that was prepared by conventional hot pressing of commercially available powders. All of the materials that were tested had relative densities greater than 97%. The resulting properties are summarized in Table 1-3. The hot-pressed sample had the highest flexural strength at  $764 \pm 46$  MPa, which was nearly 30% higher than the value measured for the material that was reaction sintered at 2050°C, which had a strength of  $528 \pm 59$  MPa. Even though the strengths were different, the average feature sizes for the reaction sintered and hot pressed specimens were similar,  $0.7 \pm 0.3$  μm and  $0.8 \pm 0.2$  μm, respectively. Possible reasons for the difference between the strengths of these materials are discussed below. The specimen sintered at 2100°C had the lowest density and strength with strength values averaging  $448 \pm 26$  MPa. When sintered at 2100°C the lower density and the larger feature size ( $2.3 \pm 0.6$  μm) both contributed to the reduced strength compared to the reaction sintered specimen sintered at 2050°C.

The elastic modulus of the hot-pressed specimen was 368 GPa, which was higher than the value of 345 GPa measured for the specimen reaction sintered at 2050°C. Tungsten has an elastic modulus of ~385 GPa and zirconium carbide has an elastic modulus of ~392 GPa, both of which are higher than the measured values for the composites [4,16]. The lower elastic modulus values of the cermets can be attributed to the small amount of porosity.

The hardness of the sample reaction sintered at 2100°C was the highest at 9.9 GPa compared to 9.2 GPa when sintered at 2050°C and 9.0 GPa when hot-pressed. The more uniform distribution of the ZrC phase in the reaction sintered samples is the likely cause of the increase in hardness compared to the hot pressed material. The larger grains of the cermet prepared by reaction sintering at 2100°C may account for increased hardness compared to the other reaction sintered material.

The fracture toughness was also compared for the reaction sintered materials. The specimens sintered at 2100°C had a slightly higher average fracture toughness at 7.8 MPa•m<sup>1/2</sup> compared to 7.1 MPa•m<sup>1/2</sup> for the material reaction sintered at 2050°C. The increase in fracture toughness in the 2100°C sintered material was most likely caused by the increase in feature size. While the difference in fracture toughness and other properties were only ~10%, the material shows potential for greater control of the properties by controlling the microstructure. The tested fracture toughness is about the same as the value reported for monolithic W, which was 7.6 MPa•m<sup>1/2</sup> [3].

Table 1-3: Mechanical properties of ZrC-W cermets made by both pressureless reaction sintering and hot pressing.

Material	Relative Density	Flexural Strength MPa	Elastic Modulus GPa	Hardness GPa	Fracture Toughness MPa√m
Reaction sintered at 2100°C	97%	448± 26	–	9.9	7.8 ± 0.3
Reaction sintered at 2050°C	98%	528± 59	345± 8	9.2	7.1 ± 0.8
Hot-pressed at 2050°C, 32MPa	99%	764 ± 46	368 ± 6	9.0	–

Griffith theory was used to estimate critical flaw sizes for some of the cermets. Using Eq. 1-2, the analysis assumed linear elastic fracture that is typical of brittle materials, which often have fracture toughness values in the range of 1-2 MPa•m<sup>1/2</sup>. The theory relates the strength ( $\sigma_f$ ) of the material to the fracture toughness ( $K_{IC}$ ) and the size of the critical flaw ( $c$ ). The Y factor is a geometric factor, which is typically assumed to be 1.98 for surface flaws and 1.128 for subsurface flaws.

$$\sigma_f = \frac{K_{IC}}{Yc^{1/2}} \quad (1-2)$$

The surface and sub-surface flaw sizes calculated for the materials produced by in situ reaction sintering at 2050°C and 2100°C are listed in Table 1-4. The calculated flaw sizes ranged from ~45 μm up to ~240 μm, which are significantly larger than the microstructural feature sizes observed in polished specimens, which were less than 3 μm.

Based on this analysis, the likely source of failure of these specimens is an agglomerate or pore located on the surface or a surface flaw caused by machining of the test specimens. The flaw may be smaller than the calculated flaws based on the high fracture toughness of the composite, and the fracture behavior may also be affected by residual stresses caused by the difference in CTE between the different materials that make up the composite.

Table 1-4: Calculated critical flaw size for reaction sintered materials.

Final Sintering Temperature	Critical flaw size (surface) ( $\mu\text{m}$ )	Critical flaw size (subsurface) ( $\mu\text{m}$ )
2050°C	46	142
2100°C	77	238

## 1.5 CONCLUSIONS

Fully dense ZrC-W cermets were formed by reaction sintering and hot pressing. Reaction sintering led to ZrC-W pellets with near fully density at two different processing temperatures. Sintering at 2050°C resulted in a higher strength (~530 MPa), but a lower hardness (~9.2 GPa) compared to the sintering at 2100°C, which resulted in a flexure strength of ~450 MPa and a hardness of ~9.9 GPa. The higher strength for the material sintered at 2050°C was attributed to a smaller feature size in the microstructure. However, the material sintered at 2100°C had a higher fracture toughness, possibly do to the larger grain size. For comparison, the material hot-pressed at 2050°C and 32 MPa had a higher strength at 764 MPa.

ZrC-W samples with a ratio of 35:65 ZrC:W can be made by different processing methods and using different densification temperatures to control the microstructure development and mechanical properties. In addition to the ability to control the microstructure, in situ reaction sintering offers the ability to make parts closer to net shape as compared to conventional hot pressing, which is limited to relatively simple geometric shapes. Near-net shape forming reduces the amount of machining required to produce finished components and, therefore, reduces production costs compared to conventional hot pressing. However, hot pressing offers improved strength. In either case, the ability to control microstructure and mechanical properties allows the material to be tailored to best suit the desired application as well as the designer's needs.

## 1.6 REFERENCES

- [1] D. R. Askeland, P. P. Phulé, *Essentials of Materials Science and Engineering*, Thomson, Ontario, Canada, 2004.
- [2] S. C. Zhang, G. E. Hilmas, W. G. Fahrenholtz, "Zirconium Carbide-Tungsten Cermets Prepared by In Situ Reaction Sintering," *J. Am. Ceram. Soc.*, 90[6], (2007) 1930-33.
- [3] G. M. Song, Y. J. Wang, Y. Zhou, "The Mechanical and Thermophysical Properties of ZrC/W Composites at Elevated Temperature," *Mater. Sci. Eng. A*, 334 (2002) 223-32.
- [4] S. W. H. Yih, C. Wang, *Tungsten: Sources, Metallurgy, Properties, and Applications*, Plenum Press, New York, 1979.
- [5] T. Leonhardt, "Properties of Tungsten-Rhenium and Tungsten-Rhenium with Hafnium carbide," *JOM*, 61[7] (2009) 68-71.
- [6] K. B. Shedd, J. W. Blossum (USGS), "Metal Prices in the United States Through 1998," U. S. Geological Survey, 2006.
- [7] E. Lassner, W. D. Schubert, *Tungsten*, Kluwer Academic/Plenum Publishers, New York, 1999.

- [8] G. W. King, H. G. Sell, "The Effect of Thoria on the Elevated-Temperature Tensile Properties of Recrystallized High-Purity Tungsten," *Trans. of the Am. Inst. of Min., Metall. and Pet. Eng.*, 233[6] (1965) 1104-13.
- [9] H. M. Yun, "Effect of Composition and Microstructure on the Creep and Stress-Rupture Behavior of Tungsten Alloy Wires at 1366-1500K," *Mater. Sci. Eng. A*, 165 (1993) 65-74.
- [10] M. Mabuchi, K. Okamoto, N. Saito, M. Nakanishi, Y. Yamada, T. Asahina, T. Igarashi, "Tensile Properties at Elevated Temperature of W-1%La<sub>2</sub>O<sub>3</sub>," *Mater. Sci. Eng. A*, 214 (1996) 174-6.
- [11] G. M. Song, Y. Zhou, Y. J. Wang, "Effect of Carbide Particles on the Ablation Properties of Tungsten Composites," *Mater. Charact.*, 50 (2003) 293-303.
- [12] M. C. Teague, G. E. Hilmas, W. G. Fahrenholtz, "Reaction Processing of Ultra-High Temperature W/Ta<sub>2</sub>C-Based Cermets," *J. Am. Ceram. Soc.*, 92[9] (2009) 1966-71.
- [13] G. M. Song, Y. J. Wang, Y. Zhou, "Thermomechanical properties of TiC particle reinforced tungsten composites for high temperature applications," *Int. J. Ref. Met. Hard Mater.* 21 (2003) 1-12.
- [14] E. Rudy, *Compendium of Phase Diagram Data*, Air Force Materials Laboratory Metals and Ceramics Division, Wright-Patterson AFB, OH, 1969, pp. 162.
- [15] M. B. Dickerson, P. J. Wurm, J. R. Schorr, W. P. Hoffman, P. G. Wapner, K. H. Sandhage, "Near net-shape, ultra-high melting, recession-resistant ZrC/W-based rocket nozzle liners via the displacive compensation of porosity (DCP) method," *J. Mater. Sci.*, 39 (2004) 6005-6015.
- [16] S. E. Landwehr, G. E. Hilmas, W. G. Fahrenholtz, I. G. Talmy, and S. G. DiPietro, "Microstructure and Mechanical Characterization of ZrC-Mo Cermets Produced by Hot Isostatic Pressing," *Mater. Sci. Eng. A*, 497 (2008) 79-86.
- [17] A. E. McHale (ed.) *Phase Diagrams for Ceramists*, Vol. X. American Ceramic Society, Westerville, OH, 1994, pp. 371.
- [18] T. Zhang, Y. J. Wang, Y. Zhou, G. M. Song, "Effect of Heat Treatment on Microstructure and Mechanical Properties of ZrC Particles Reinforced Tungsten-Matrix Composites," *Mater. Sci. Eng. A*, 512 (2009) 19-25.

## II. DENSIFICATION AND MICROSTRUCTURE OF ZrC-W CERMETS

Melissa M. Giles, S. C. Zhang, W.G. Fahrenholtz, G.E. Hilmas

### 2.1 ABSTRACT

ZrC-W cermets with ZrC contents ranging from 35 vol% to 65 vol% were prepared by in situ reaction sintering and hot pressing. Densification studies were performed at temperatures ranging from 1800°C to 2100°C. The cermets with the highest relative densities were characterized and hardness values were measured. The hardness was found to increase with increasing ZrC content. The highest hardness was measured for 65 vol% ZrC produced by hot pressing at 13.2 GPa. The lowest measured hardness was produced at 35 vol% ZrC with a hardness of 9.0 GPa. Altering the composition allows properties such as density and hardness to be tailored for specific applications.

### 2.2 INTRODUCTION

Ceramic-metal composites, also known as cermets, can combine the desirable properties of ceramics and metals into a single composite material. The desire for better materials for specific applications has driven the development of new materials [1]. Metals such as tungsten have good room temperature mechanical properties, such as strength and hardness. However, those properties decrease as temperature increases and can reach a point where the material is too weak and will not maintain strength or even shape in some applications [2,3]. Ultra high temperature ceramics (UHTCs), such as ZrB<sub>2</sub> and HfB<sub>2</sub> [4,5], retain the majority (>50%) of the room temperature strength at elevated temperatures and thermal stability at temperatures above 1600°C [6,7], but lack the

formability and have unwanted characteristics such as being mechanically brittle [8]. The combination of these materials can result in a material with a desired combination of properties allowing for use in areas where the advancement in technology is limited by the material. Applications that involve high temperature environments often also involve corrosive environments. Areas such as rocket nozzles, combustion chambers in engines, or tubing in nuclear reactors all see harsh environments where elevated temperatures are encountered along with other factors such as high humidity or corrosive gases [3,9]. Cermets can also offer improved stability against corrosion.

Tungsten (W) is the highest melting refractory metal (3422°C). However, the strength of tungsten decreases drastically, losing about 60% of its room temperature strength by 1000°C and decreasing further above 1000°C [3]. Alloys of tungsten have been used to try to improve the high temperature properties; however, alloying with materials such as rhenium can increase the cost of the material with only minimal improvement in properties [2,10]. Adding ceramic particles such as HfC, ZrO<sub>2</sub>, ZrC and TiN can also improve elevated temperature strength. For example, 20 vol % ZrC has been added to tungsten to form a cermet with a room temperature flexural strength of 1046 MPa [11]. However, the decrease in strength was drastic below 1000°C, with the largest decrease, from ~1650 MPa yield strength to ~600 MPa, happening before 600°C [11]. The addition of ZrC stabilizes strength between 600 and 1000°C. However, the flexure strength was around 600 MPa, about half of the initial strength [11]. Song tested specimens of 30 vol% ZrC in a tungsten matrix. The reported strength at room temperature was ~705 MPa. Further, strength increased with temperature and reached ~830 MPa at 1000°C and maintained at least 810 MPa to 1200°C [9].



Previous research has shown the potential for increasing the strength of W through alloying additions. Further, adding carbide particles such as TiC or ZrC has also been reported to improve strength as well as performance in such areas as ablation behavior [12]. Carbides of transition metals form limited solid solutions with W, which increases strength at interfaces between the two materials and improves the strength and toughness of the cermet. The previous work reported on ZrC-W composites shows the promise of this material for use in high temperature applications with corrosive environments.

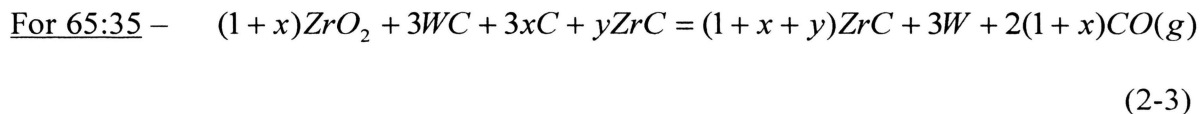
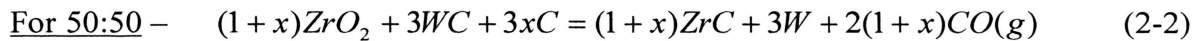
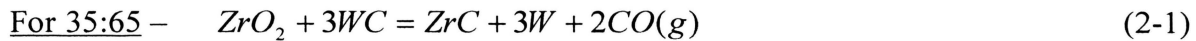
The high melting point of ZrC (3540°C) is similar to that of W (3422°C). In addition, the thermal expansion coefficient (CTE) of ZrC is relatively low,  $4.0 \times 10^{-6}/^{\circ}\text{C}$ , which is similar to the value of  $4.5 \times 10^{-6}/^{\circ}\text{C}$  reported for W [13]. The similarity of the thermal expansion coefficient minimizes thermal residual stress formation, which reduces the potential for failure during thermal cycling. ZrC also has a lower density ( $6.74\text{g}/\text{cm}^3$ ) than W ( $19.25\text{g}/\text{cm}^3$ ), which decreases the density of ZrC-W cermets compared to W and makes them more appealing for aerospace applications. For aerospace applications added weight can result in added fuel costs or reduced payload [14]. The areas of interest for high temperature components in aerospace are often in the engine where increasing the temperature of operation results in increased efficiency; however, if the weight of the component counteracts the gain in efficiency then it is not economical to switch.

The purpose of this study was to investigate the effect of varying ZrC content on the microstructure and properties of ZrC/W cermets. The ZrC contents that were considered were 35 vol%, 50 vol%, and 65 vol%.

## 2.3 EXPERIMENTAL PROCEDURE

Cermets with three different ZrC contents were produced using either in situ reaction sintering or hot pressing. The three cermet compositions were: 1) 35 vol% ZrC and 65 vol% W, which is designated 35:65; 2) 50 vol% ZrC and 50 vol% W, which is designated 50:50; and 3) 65 vol% ZrC and 35 vol% W, which is designated 65:35. For all compositions, the ZrC content is given first in the designation.

**2.3.1 In Situ Reaction Sintering.** Commercial powders were used as the starting materials. The WC (< 1 $\mu$ m, 99% purity, Cerac Inc., Milwaukee, WI), ZrO<sub>2</sub> (-325 mesh, >99% purity, Alfa Aesar Chemical Co., Ward Hill, MA) and ZrC (-325 mesh, >99.5% purity, Cerac Inc.) were batched to achieve the desired ratios as described by Reactions 2-1, 2-2 and 2-3.



The first reaction (Reaction 2-1) is termed “stoichiometric” and yields 35 vol% ZrC and 65 vol% W. The second reaction produced a 50:50 ZrC:W ratio and was obtained by adding phenolic resin to increase the carbon content and additional ZrO<sub>2</sub> to increase the Zr content. When the phenolic resin was charred, it reduced to carbon, which, along with the additional amount of ZrO<sub>2</sub>, shifted the molar ratio of ZrO<sub>2</sub> to WC by the factor x shown in Reaction 2-2. To produce the desired 50:50 ratio, x was set to

0.8. To shift the ZrC:W ratio further and obtain a higher volume fraction of ZrC than W for the 65:35 composition, extra carbon, ZrO<sub>2</sub> and ZrC were added to the mixture (Reaction 2-3). To produce the 65:35 ZrC:W ratio, the reaction variables were set to  $x = 1.05$  and  $y = 1.45$ , which yielded nominally 65 vol% ZrC and 35 vol% W.

Prior to reaction, ZrO<sub>2</sub> and ZrC powders were attrition milled (Model 01-HD, Union Process, Akron, OH) using yttria stabilized zirconia or WC media, respectively, in ethanol for 2 hours to reduce the particle size. After milling, the average particle size of the ZrO<sub>2</sub> ( $d_{50}$ ) measured using laser light scattering (Microtrack model S3500, Microtrac Inc., York, PA) was 0.42  $\mu\text{m}$ . The attrition milled ZrO<sub>2</sub> (and attrition milled ZrC for Reaction 2-3) was mixed with as-received WC powder by ball milling for 48 hours in acetone using WC media. In addition, 5 mg of dispersant (DISPERBYK-110, BYK-Chemie Co., Wesel, Germany) was added per square meter of surface area of the powders. The surface area was estimated from the measured diameter assuming round particles. After mixing, the desired amount of soluble phenolic resin (GP 2074, Georgia Pacific CO., Atlanta, GA) was added (Table 2-1). Phenolic resin is a carbon precursor that is soluble in organic solvents, but precipitates to coat the solid powder particles when the solvent is removed [15]. The powders were mixed for one hour and then dried while continuously stirring using a magnetic stir bar on a hot plate that was kept below 100°C. The dried powders were crushed with a mortar and pestle and sieved to -80 mesh.

Cylindrical pellets 1.3 cm (0.5 inch) in diameter were prepared for a sintering study. Pellets were formed by uniaxially pressing to 3.4 MPa (500 psi) followed by cold isostatic pressing to 207 MPa (30 ksi).

The charring of the phenolic resin to produce excess carbon for Reactions 2-2 and 2-3 was done after the pellets were pressed. The pressed pellets were heated in Lindberg box furnace fitted with an Inconel retort under flowing argon to 900°C following the furnace schedule shown in Figure 2-1. The weight yield of carbon from phenolic resin after charring was 40%, based on thermal gravimetric analysis. Table 2-1 lists the values of  $x$ , the wt% of phenolic resin added and the wt% of carbon that resulted for Reactions 2-2 and 2-3.

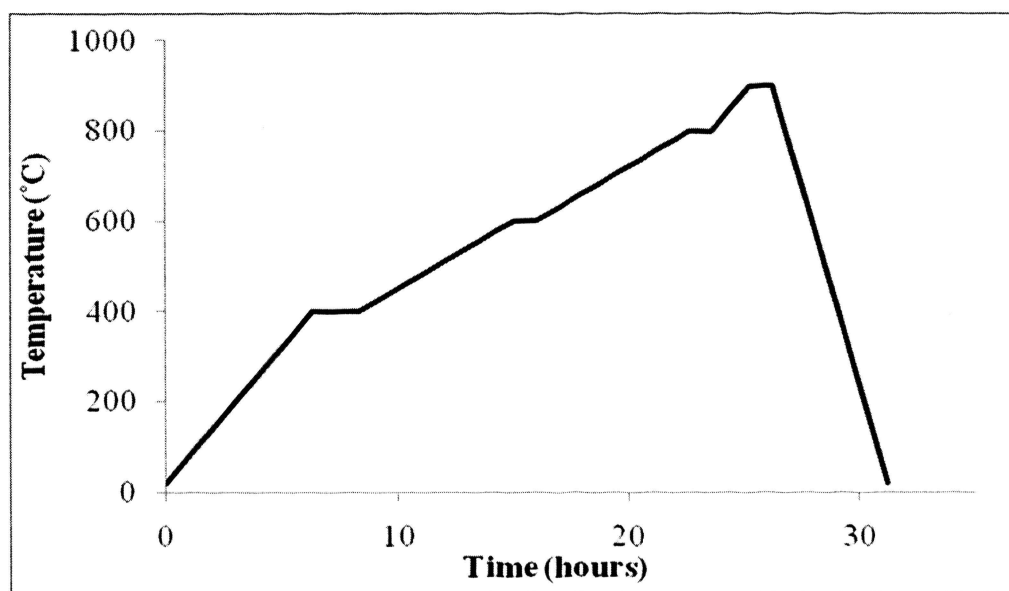


Figure 2-1: Phenolic resin charring schedule.

Table 2-1: The values of  $x$  for Reactions 2-2 and 2-3, and the corresponding amounts of phenolic resin added along with the predicted carbon yield.

Composition	Value of $x$ in Reaction	Wt.% Phenolic Resin	Wt.% Carbon
50:50	0.8	8.5	3.4
65:35	1.05	9.25	3.7

After charring, pellets were sintered at temperatures ranging from 1900°C and 2150°C for a densification study. Sintering was conducted in a graphite element furnace 3060-FP20, Thermal Technology, Santa Rosa, CA). The furnace was heated under vacuum (~20 Pa) at 10°C per minute from room temperature to 1850°C. Isothermal holds were used at 1250°C for 1 hour (1400°C for the 50:50 ratio) and 1650°C for 1 hour to allow recovery of the vacuum. For the 65:35 ratio, the ramp rate between 1250°C and 1650°C was reduced to 5°C/min based on the additional volume of CO produced from the extra ZrO<sub>2</sub> and C in that reaction mixture. An additional hold at 1850°C for 1 hour was used for all materials to switch the furnace atmosphere from vacuum to flowing argon at a slight over pressure of approximately 20 kPa (gauge pressure). After holding at 1850°C, the furnace was heated to the final sintering temperature at a rate of 20°C/min and held for 4 hours, for all samples.

**2.3.2 Hot Pressing.** Pellets were prepared for conventional hot pressing from commercially available ZrC (-325 mesh, > 99.5% purity, Cerac Inc.) and W (1-5 μm, >99.9% purity, Alfa Aesar, Ward Hill, MA) powders. The ZrC was attrition milled for two hours using WC milling media. The ZrC and W were then batched to obtain mixtures containing 35 vol%, 50 vol% or 65 vol% ZrC. The batched powders were mixed by ball milling for 24 hrs in ethanol with 1 wt% dispersant (DISPERBYK-110). The powders were dried, crushed using a mortar and pestle, and sieved to -80 mesh. The powders were then packed into a 4.5 cm (1.75 in) diameter graphite die lined with graphoil that had been coated with a thin layer of boron nitride (BN) spray to minimize reaction between the powder and the die.

Hot press runs for the densification study used a ramp rate of 20°C/min under vacuum to 1650°C where the furnace was held at temperature for 1 hour to allow recovery of the vacuum to the nominal level of ~20 Pa. After the one hour hold, the atmosphere was switched to flowing argon and pressure was applied to 32 MPa. Then the temperature was raised by 20°C/min to the final sintering temperature, which ranged from 1700°C to 2050°C. The specimens were held at the final sintering temperature for 10 min after the ram travel ceased. The total time at temperature averaged 1 hr. The furnace was then cooled at ~20°C/min, and the pressure was released once the furnace cooled below 1650°C.

**2.3.3 Characterization and Testing.** Archimedes' method was used to measure the bulk densities of sintered specimens. Water was used as the immersion medium. The theoretical densities of the different compositions were calculated from the amounts of ZrC and W expected in the final products based on the stoichiometries of Reactions 2-1, 2-2, and 2-3. The relative densities were calculated by dividing the measured bulk density by the estimated theoretical density. For comparison, the densities were estimated for the three different compositions relative to pure W.

Table 2-2: Density comparison for the three different compositions for in situ reaction sintered (Rxn) and hot-pressed (HP) samples.

Composition	Theoretical Density (g/cm <sup>3</sup> )	Compared to pure W (less than %)	Measured Density (g/cm <sup>3</sup> )		Relative Density (%)	
			Rxn	HP	Rxn	HP
35:65	14.9	22.6	14.5	14.7	97.6	99.0
50:50	13.0	32.5	12.5	13.0	95.0	100.0
65:35	11.1	42.3	—	11.2	—	100.0

The Gibbs free energy changes for reactions were calculated using HSC Chemistry 5.11 software (HSC Chemistry, Outokumpu Research Oy, Pori, Finland). The calculations assumed that the measured furnace pressure was equal to the partial pressure of the gaseous reaction product, CO.

X-ray diffraction (XRD;  $\theta$ - $\theta$  type XDS200 X-ray diffractometer XDS 2000, Scintag Inc., Cupertino, CA) analysis was used to identify the phases present after densification. Specimens were prepared by crushing and grinding pellets produced by in situ reaction sintering or hot pressing. The scans were performed on packed powder mounts using Cu-K $\alpha$  radiation in step mode using a step size of 0.03 deg and a count time of 2 seconds.

Microstructures were analyzed using scanning electron microscopy (SEM; S570 or S4700, Hitachi, Tokyo, Japan). The top of the pellets were ground flat using a 125  $\mu\text{m}$  grit polishing pad. The ground surfaces were polished using diamond slurries down to 0.25  $\mu\text{m}$  for microstructure analysis. Image analysis was performed using image analysis software (Image J, National Institutes of Health, Washington, DC) to determine feature size and area fractions.

The same specimens used for microstructure analysis were used for hardness testing and were polished to 0.25  $\mu\text{m}$  using a diamond grit polishing pad. Hardness was measured using a minimum of 10 Vickers' indents using a 4.91N load and a dwell of 10 seconds (Duramin 5, Struers, Westlake, OH) following ASTM Standard C1327-03.

## 2.4 RESULTS AND DISCUSSION

**2.4.1 Thermodynamic Considerations.** Thermodynamic calculations for the different reactions showed that the temperatures at which the reactions became favorable shifted to lower values as the ZrC content of the cermets increased (Figure 2-2). The Gibbs free energy calculations were completed assuming the reactions taking place were only Reactions 2-1, 2-2 and 2-3. The temperatures at which the reactions became favorable are listed in Table 2-3. Reaction 2-1 had the highest initiation temperature at 1956°C, while Reaction 2-3 had the lowest reaction temperature at 1811°C, which is a difference of over 100°C.

The temperatures at which the reactions became favorable shifted to lower temperatures when the effects of system pressure were considered. As described in the procedure, in situ reaction sintering was conducted at a nominal furnace pressure of ~20 Pa, which was measured using a thermal conductivity vacuum gage on the furnace. For the calculations, the measured furnace pressure was assumed to be the partial pressure of the gas (CO) produced by the reactions. Because the furnace pressure would be the maximum possible pressure of CO gas, the temperatures estimated using the calculations represent an upper limit for the temperatures at which the reactions would become favorable. Table 2-3 lists the temperatures at which Reactions 2-1, 2-2, and 2-3 are favorable at standard pressure and the nominal furnace pressure. The reaction temperatures decreased when changing from standard pressure to the nominal pressure in the furnace (~20 Pa), with all of the reactions becoming favorable around 1250°C, which is the temperature of the first isothermal hold in the processing cycle. An increase in furnace pressure was observed at 1250°C, which was likely due to the production of CO



(g) as a product of the reactions at this temperature. Based on the calculations and observations of variations in the furnace pressure during processing, the first isothermal holds used for processing the 35:65 and 65:35 compositions were placed at 1250°C. Holding the furnace at this temperature for one hour was sufficient for the vacuum to return to the nominal level after gas evolution associated with the reactions was complete. For Reaction 2-2, the initial furnace pressure increase occurred around 1400°C, as compared to the other compositions, which had observed pressure increases at 1250°C. The difference in the initiation temperature for Reaction 2-2 may be due to the composition, as this reaction has the lowest amount of  $ZrO_2$  relative to the other reactants. As a result, the isothermal hold temperature for this composition was increased to 1400°C with a hold time of one hour. In addition to the holds described above, all of the compositions were also held at 1650°C for one hour due to another increase in the furnace pressure at this higher temperature. The vacuum change at 1650°C suggests that the reactions did not go to completion at the lower temperature, even though they had initiated there.

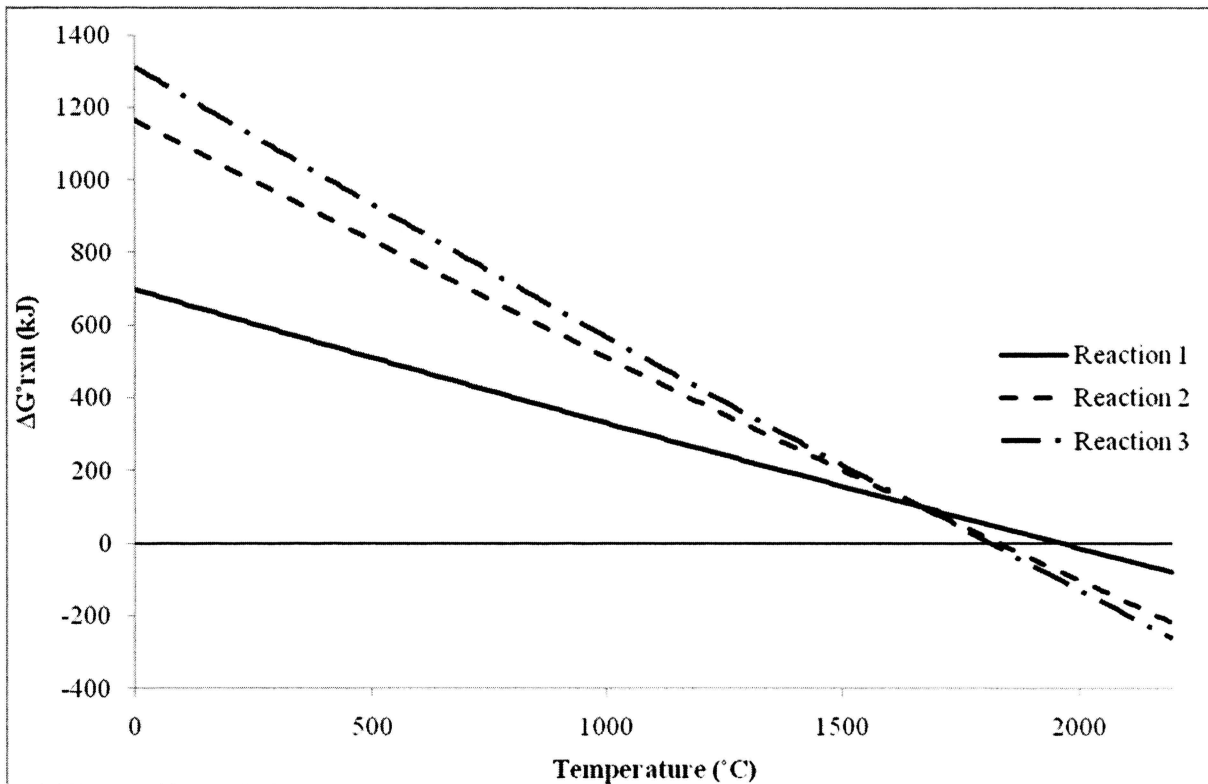


Figure 2-2: Standard state change in Gibbs free energy ( $\Delta G_{\text{rxn}}^{\circ}$ ) for Reactions 1, 2, and 3.

Table 2-3: Predicted reaction temperatures for under vacuum and at atmospheric pressure of Reactions 2-1, 2-2, and 2-3.

Pressure (Pa)	Temperature (°C)		
	Reaction 1	Reaction 2	Reaction 3
20	1317	1223	1208
101,325	1956	1831	1811

Analysis of XRD patterns (Figure 2-3) showed that the main phases present after sintering at 1800°C or above were ZrC and W. As the amount of ZrC in the cermet increased, the ZrC peak intensity increased. In addition, the ZrC peaks were shifted to higher angles than reported in the catalog (JCPDS card 35-0784 for ZrC) for all

specimens. The (311) peak for ZrC is reported to be at  $65.97^\circ$ , but was shifted for the 35:65 material sintered at  $2050^\circ\text{C}$  to  $66.24^\circ$ , a shift of  $0.27^\circ$ . The shifts in the ZrC peak positions were due to W substitution into the ZrC lattice, which formed (Zr,W)C solid solutions. The amount of W that had substituted into the ZrC was estimated by comparing the measured lattice parameter to that from ZrC reported for pure ZrC. The estimates were made assuming a linear decrease in lattice parameter from 4.693 for pure ZrC assuming covalent radii of  $1.57\text{\AA}$  for Zr and  $1.38\text{\AA}$  for W [16]. Table 2-4 compares the lattice parameters and the amounts of W predicted to be in the ZrC phase. For comparison, the solubility limit of W in ZrC is  $\sim 7$  mol%, which was reported by McHale [17] for arc melted ZrC and W.

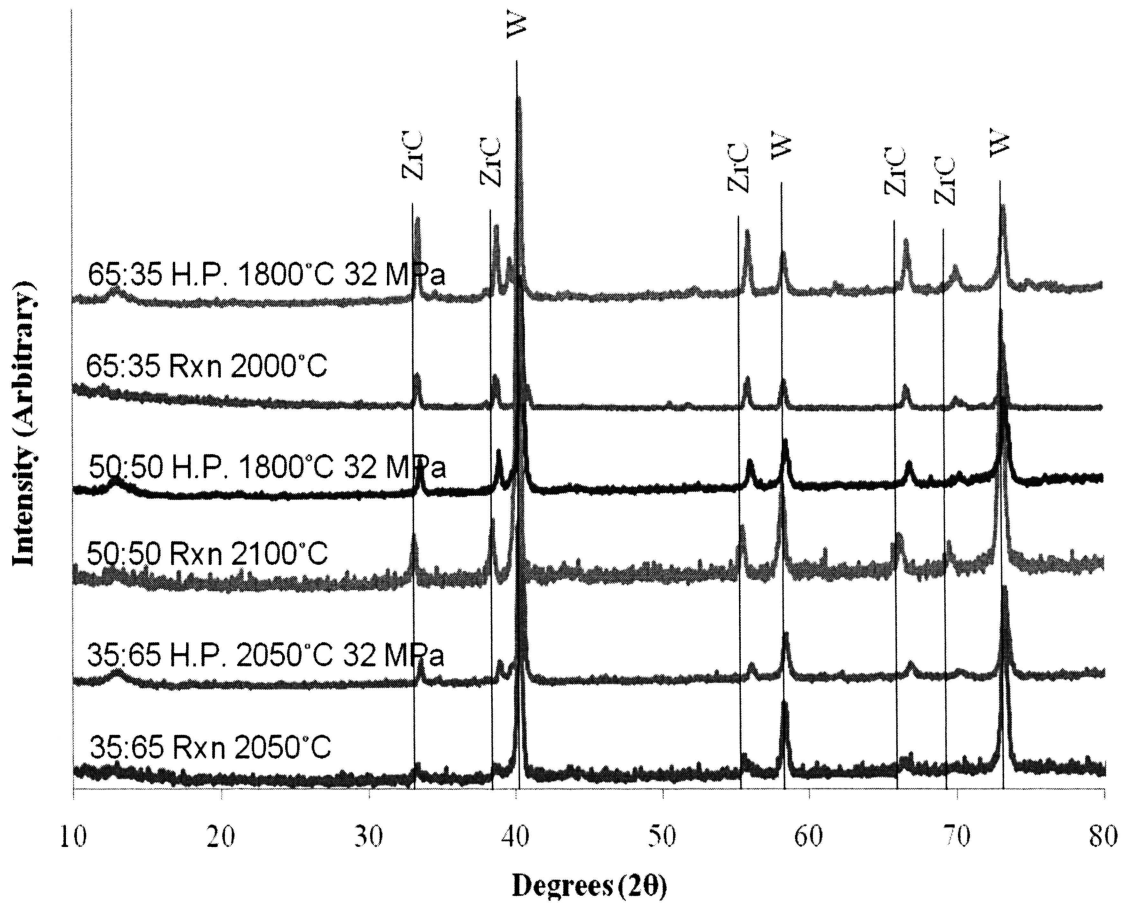


Figure 2-3 XRD patterns for specimens produced by in situ reaction sintering (Rxn) or hot pressing (HP) at various temperatures.

It appears that the amount of W in solid solution in ZrC decreased with increasing ZrC in the hot-pressed and reaction sintered specimens, due to the decrease in available W. The exception being the 50:50 composition produced by reaction sintering which demonstrated a much lower amount of W in solid solution (approximately 1 mol% W). The main cause for the lower solid solution in this composition could be the decrease in

surface area between the ZrC and W phases with the larger microstructure. The larger microstructure is attributed to the grain growth that occurred above 2050°C.

Table 2-4 Lattice parameters of ZrC and the corresponding amount of W in solid solution (ss) for the highest density samples both produced by in situ reaction sintering (Rxn) and hot pressing (HP).

Composition	Lattice parameter (Å)	W in ss (mol%)*
Pure ZrC	4.69	0.0
Rxn ZrC 65 vol% W	4.65	4.4
HP ZrC 65 vol% W	4.65	4.6
Rxn ZrC 50 vol% W	4.68	1.4
HP ZrC 50 vol% W	4.64	5.4
Rxn ZrC 35 vol% W	4.63	6.8
HP ZrC 35 vol% W	4.64	5.6

\*Values are  $\pm 1$  mol%.

**2.4.2 Densification.** The specimens made by in situ reaction sintering showed a trend of increasing density with increasing sintering temperature (Figure 2-4). The in situ reaction sintered specimens with 35 vol% ZrC peaked at a density of 97.6% at 2050°C whereas the specimens with 50 vol% ZrC peaked with a density of 95.0% at 2100°C. The reaction sintered specimens containing 65 vol% ZrC were not tested using the Archimedes' method due to severe cracking in the final sintered specimens. Full densification was achieved for all ZrC:W ratios by hot pressing. Hot pressing resulted in densification at lower sintering temperatures with increasing ZrC content. For each ZrC:W ratio, full density was achieved at lower temperatures than for specimens produced by in situ reaction sintering. For the 65:35 and 50:50 compositions, full density

(> 99% relative density) was attained at 1800°C and 32MPa. The 35:65 specimen reached a density of 97.8% at 1900°C and 99.0% at 2050°C. SEM analysis, to be discussed later, was also used to estimate the final relative density. All specimens were able to reach full density (no visible porosity) when produced by hot pressing, only Reaction 2-1 was able to produce specimens with a relative density over 98% using the in situ reaction sintering process. Further process optimization is needed for specimens produced using Reactions 2-2 and 2-3 to reach full density.

The decrease in relative density with increasing ZrC content is likely due to the significant volume changes associated with the reaction. Densification requires not only the elimination of porosity from the pressed pellets, but must also overcome a significant volume contraction associated with the chemical reaction. The volume changes predicted for Reactions 2-1, 2-2, and 2-3 were 27 vol%, 40 vol% and 35.2 vol%, respectively. Outgassing associated with CO (g) formation is also a factor in the densification process in that retention of vapor species inside pellets could lead to the formation of entrapped porosity or, in extreme cases, rupture of the specimens. The combination of the volume change due to reaction and that due to elimination of porosity makes densification of specimens with higher ZrC contents more difficult. The potential problems associated with formation of gaseous species can often be mitigated using slow heating rates and extended isothermal holds in temperature ranges where gaseous species are generated. However, the densification conditions used in this study did not eliminate these problems.

The pressed pellets had relative densities in the range of 50 to 60% (50% to 40% porosity), making the total volume change required for complete reaction and densification range from ~56% for Reaction 2-1 to ~70% for Reactions 2-2 and 2-3.

Increasing the amount of  $ZrO_2$  in the precursors for Reactions 2-2 and 2-3 leads to an increase in the amount of  $CO$  (g) formed by the reactions; every mole of  $ZrO_2$  produces 2 moles of  $CO$  (g) upon reaction to  $ZrC$ . The isothermal holds in the processing cycles were designed to control the rate of gas formation to minimize the possibility of rupturing specimens due to rapid generation of internal pressure.

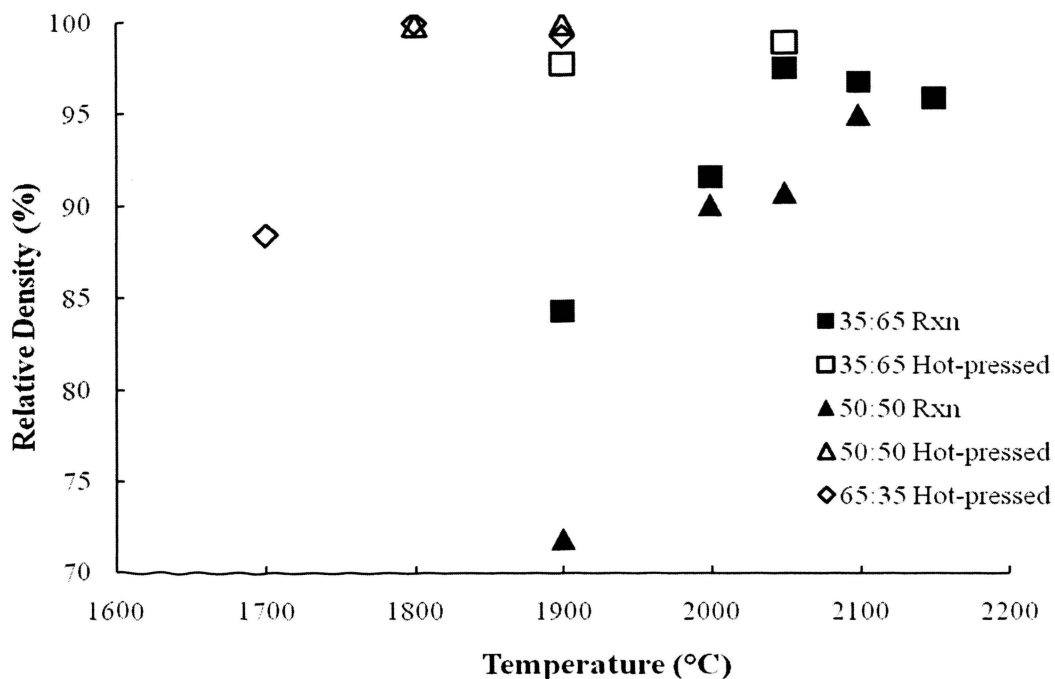


Figure 2-4: Relative density as a function of sintering or hot pressing temperature.

**2.4.3 SEM Analysis.** The SEM images (Figure 2-5a-c) compare the microstructures of composites with increasing  $ZrC$  content prepared by reaction sintering. All of the reaction sintered compositions appeared to have a two phase, interpenetrating type microstructure [18] in which both the  $ZrC$  and  $W$  phases are continuous.

The micrographs indicate that the materials produced by in situ reaction sintering had high relative density (>95% for 35:65 and 50:50). The small volume fraction of porosity was mainly located within the ZrC phase, primarily on ZrC-ZrC grain boundaries, but sometimes appearing at ZrC-W phase boundaries. The specimens formed by Reactions 2-2 (b) and 2-3 (c) showed areas of concentrated porosity surrounded by areas that were fully dense (Figure 2-6). The larger features in b were due to an increase in grain growth that occurred between 2050°C and 2100°C.

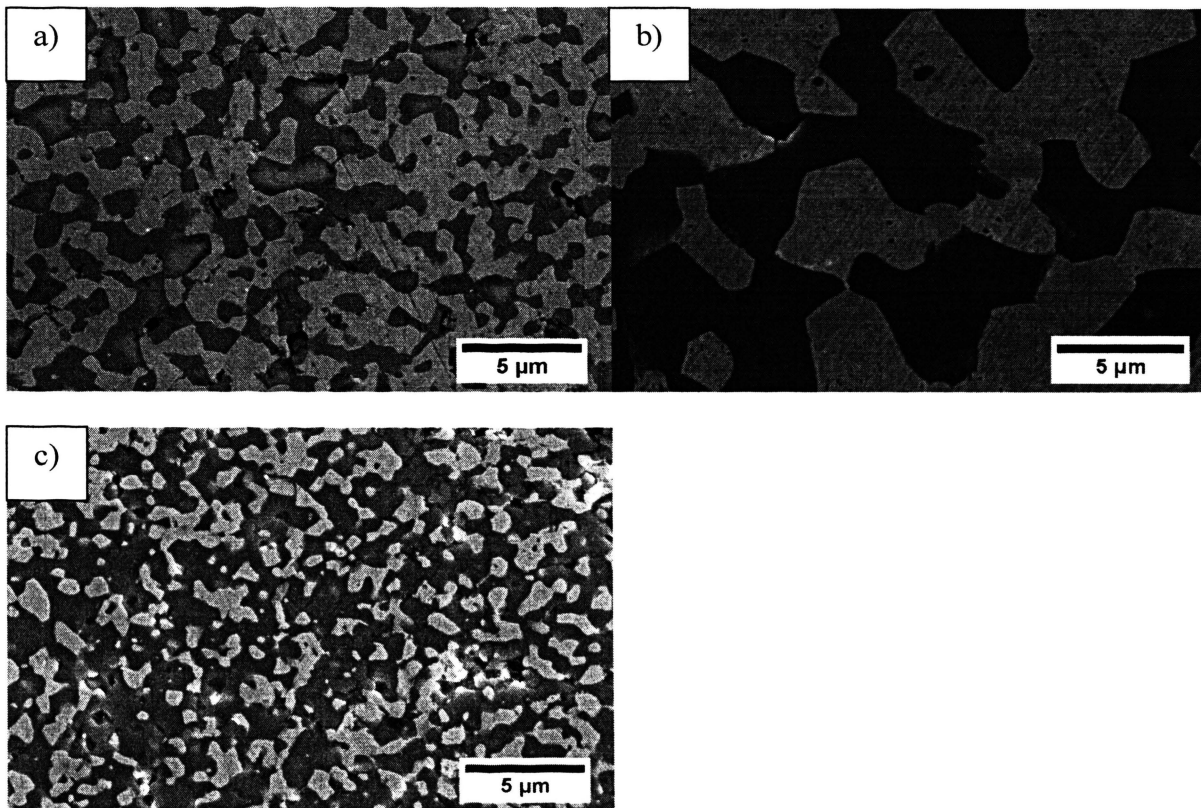


Figure 2-5: SEM micrographs comparing the microstructure of reaction sintered specimens of varying ZrC content a) 35 vol% ZrC (2050°C), b) 50 vol% ZrC (2100°C), c) 65 vol% ZrC (2000°C).



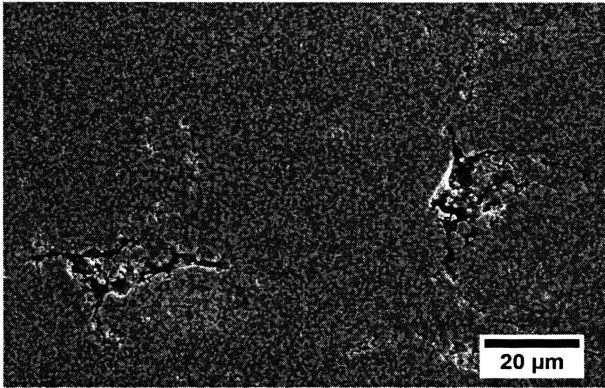


Figure 2-6: SEM microstructure of reaction 2-3 cross section.

Figure 2-7 shows SEM images of the specimens produced by conventional hot pressing. The specimens were made to have nominally the same compositions as those produced by in situ reaction sintering. The hot-pressed compositions showed a tendency for clustering of the ZrC phase as compared to the uniform interpenetrating structure observed for the reaction sintered compositions. The clustering was likely due to agglomeration before hot pressing. In comparison, for all hot-pressed specimens the features were clustered and larger (5-10  $\mu\text{m}$ ) in the hot-pressed specimens compared with the reaction sintered specimens.

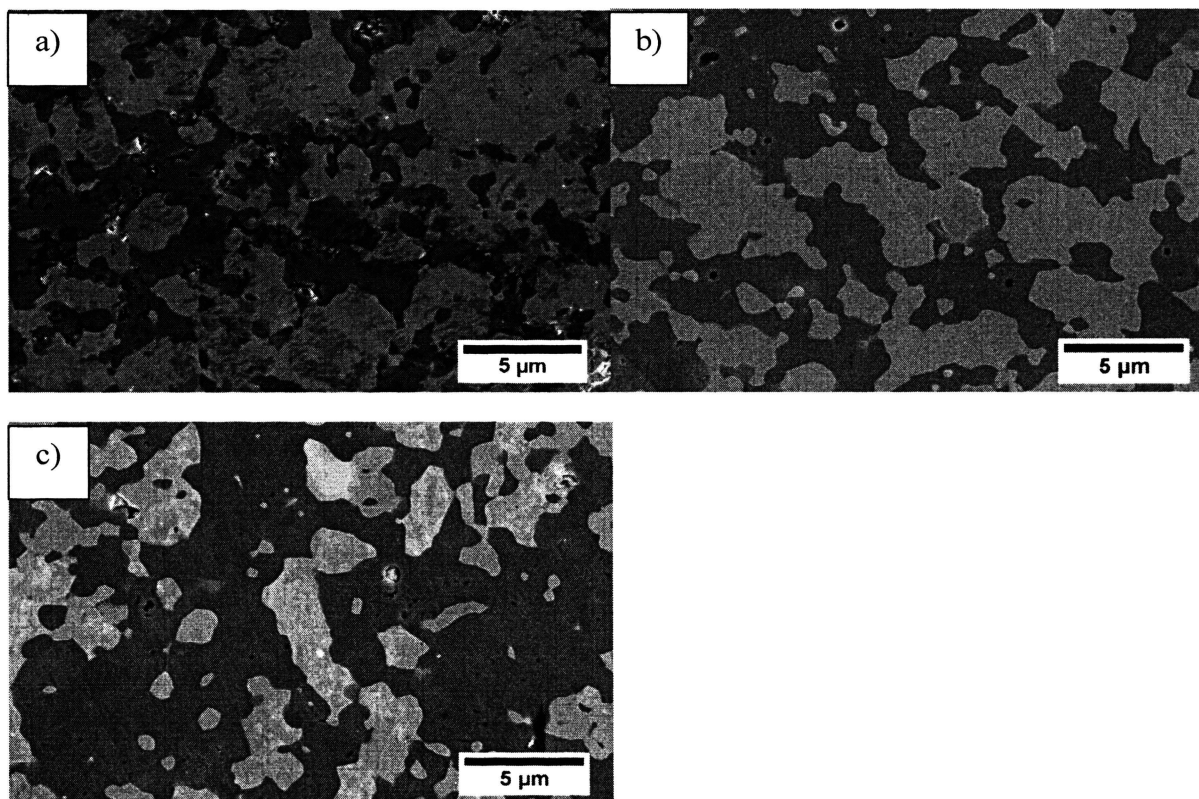


Figure 2-7: SEM micrographs comparing the microstructure of hot pressed specimens of varying ZrC additions a) 35 vol% ZrC (2050°C 32 MPa), b) 50 vol% ZrC (1900°C 32 MPa), c) 65 vol% ZrC (1800°C 32 MPa).

Table 2-5 lists the 6 different materials that are shown in the SEM images (Figure 2-5 and Figure 2-7) and the corresponding measured size of the ZrC regions. The feature size was dependent on the densification temperature more than the sintering method. However, the hot-pressed specimens seemed to have larger features than the in situ reaction sintered specimens when the processing temperatures were the same. The features of the 50:50 reaction specimens are roughly the same size (Table 2-5) as the features or clusters in the hot-pressed sample with the agglomerates measuring  $3.3 \pm 0.8$  μm.

Table 2-5: Feature size analysis.

Composition	Average	Standard Deviation
Rxn 1: 2050	0.74	0.25
HP 1: 2050	0.78	0.23
Rxn 2: 2100	2.79	0.94
HP 2: 1800	0.70	0.29
Rxn 3: 1900	0.57	0.21
HP 3: 1800	0.77	0.30

**2.4.4 Hardness.** Vickers hardness increased with increasing ZrC content for both processes. ZrC is the harder phase in the ZrC:W cermets with a reported hardness of 25.5 GPa [19] while W has a reported hardness of 3.4 GPa. [20] With only 35 vol% ZrC additions the hardness increased to ~9 GPa for both reaction and hot-pressed specimens.

Table 2-6 lists the values for the tested hardness for all specimens. The reaction sintered 65:35 specimen was not tested do to the amount of cracking and porosity in the final specimens. The in situ reaction sintered specimens were harder than the hot-pressed materials. The maximum hardness of the specimens tested was 13.2 GPa for 65 vol% ZrC produced by hot pressing. With 35 vol% ZrC additions the hardness is ~3 times that of pure W and with 65 vol% ZrC additions the hardness is ~4 times that of pure W.

Table 2-6: Hardness.

Hardness	In Situ Reaction Sintered	Hot-Pressed
35:65	$9.2 \pm 0.7$ GPa	$9.0 \pm 0.3$ GPa
50:50	$11.3 \pm 1.3$ GPa	$10.3 \pm 0.6$ GPa
65:35	—	$13.2 \pm 0.6$ GPa

The hardness data was compared to a model developed by Lee and Gurland, (Equation 2-4) that is an adjustment to the rule of mixtures. The hardness of the composite ( $H_C$ ) is determined by the hardness of the carbide, in this case ZrC ( $H_{ZrC}$ ), and the hardness of the metal, W ( $H_W$ ) in conjunction with the volume fraction of the carbide ( $V_{ZrC}$ ) and the contiguity ( $C$ ). The hardness values of ZrC and W are based on the previously reported values (shown in Figure 2-8 as  $H_0$ ), the hardness of ZrC is taken to be 25.5 GPa and the hardness of W is 3.4 GPa as previously reported [19,20]. The contiguity factor changes with increasing ZrC content so  $C$  was determined based on an average of the three ZrC amounts in the study. The hardness with relation to the amount of ZrC (Figure 2-8), as shown compared to the Lee and Gurland model (Equation 2-4). The model is a good approximation for the ZrC range from 35 vol% to 65 vol% with deviations at the high ZrC content end of the Lee and Gurland fit line.

$$H_C = H_{ZrC}V_{ZrC}C + H_W(1 - V_{ZrC}C) \quad (2-4)$$

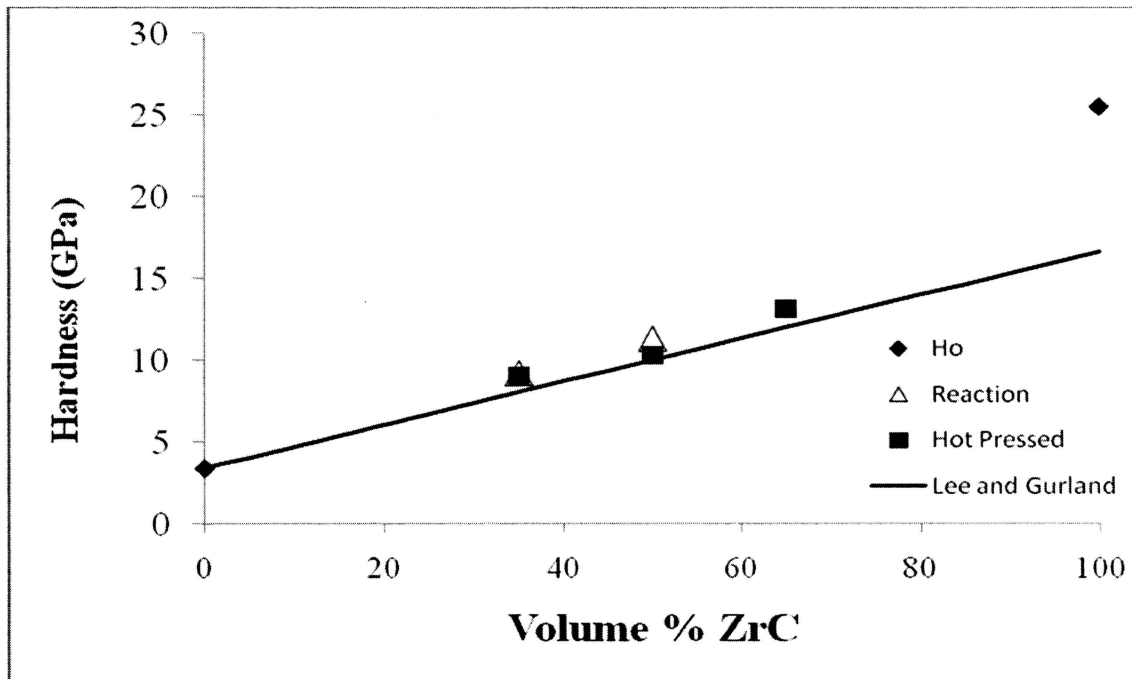


Figure 2-8: Hardness in relation to ZrC content.  $H_0$  is the hardness of ZrC and W.

## 2.5 CONCLUSIONS

ZrC-W cermets with ZrC contents of 35, 50, 65 vol% were prepared by hot pressing and in situ reaction sintering. The volume ratios of 35 vol% and 50 vol% were densified fully. The ZrC content of 65 vol% has shown promise for reaction processing methods of densification. All composites showed formation of (Zr, W)C solid solution.

The hardness showed an increase with increasing ZrC additions. In general the reaction sintered composites showed a higher measured hardness than the composites made by hot pressing. The hot pressed 35 vol% ZrC specimen had a hardness of 9 GPa compared to the hot pressed specimen with 65 vol% ZrC that had a hardness of 13 GPa

## 2.6 REFERENCES

- [1] J. R. Tinklepaugh and W. B. Crandall, *Ceremets*, Reinhold Publishing Corp., New York, 1960.
- [2] E. Lassner and W. D. Schubert, *Tungsten*. Kluwer Academic/Plenum Publishers, New York, 1999.
- [3] Stephen W. H. Yih and Chun T. Wang, *Tungsten: Sources, Metallurgy, Properties, and Applications*. Plenum Press, New York, 1979.
- [4] S. R. Levine, E. J. Opila, M. C. Halbig, J. D. Kiser, M. Singh, J. A. Salem, "Evaluation of ultra-high temperature ceramics for aeropulsion use," *J. Eur. Ceram. Soc.* 22 (2002) 2757-67.
- [5] R. Loehman, E. Corral, H. P. Dumm, P. Kotula, R. Tandon, "Ultra High Temperature Ceramics for Hypersonic Vehicle Applications," Sandia Report, Sandia National Laboratories 2006.
- [6] X. X. Bu, Y. W. Bao, "Mechanical Properties Evaluation of Ultra-high Temperature Ceramics," *Key Engineering Materials* 368-372 (2008) 1791-1794.
- [7] F. Monteverde, C. Melandri, S. Guicciardi, "Microstructure and mechanical properties of an HfB<sub>2</sub> + 30 vol.% SiC composite consolidated by spark plasma sintering," *Mater. Chem. Phys.* 100 (2006) 513-19.
- [8] Askeland, Donald R. Pradeep P. Phulé, *Essentials of Materials Science and Engineering*, Thomson, Ontario, Canada, 2004.
- [9] G. M. Song, Y. J. Wang, and Y. Zhou, "The mechanical and thermophysical properties of ZrC/W composites at elevated temperature," *Material Science and Engineering A.* 334, 223-32 (2002).
- [10] S. C. Zhang, G. E. Hilmas, and W. G. Fahrenholtz, "Zirconium Carbide-Tungsten Cermets Prepared by In Situ Reaction Sintering," *J. Am. Ceram. Soc.*, 90[6] 1930-33 (2007).
- [11] T. Q. Zhang, Y. J. Wang, Y. Zhou, and G. M. Song, "Effect of heat treatment on microstructure and mechanical properties of ZrC particles reinforced tungsten-matrix composites," *Material Science and Engineering A.* 512, 19-25 (2009).
- [12] G. M. Song, Y. Zou, and Y. J. Wang, "Effect of carbide particles on the ablation properties of tungsten composites," *Materials Characterization*, 50, 293-303 (2003).

- [13] M. B. Dickerson, P. J. Wurm, J. R. Schorr, W. P. Hoffman, P. G. Wapner, K. H. Sandhage, "Near net-shape, ultra-high melting, recession-resistant ZrC/W-based rocket nozzle liners via the displacive compensation of porosity (DCP) method," *J. Mater. Sci.*, 39 (2004) 6005-6015.
- [14] Donald R. Askeland and Pradeep P. Phulé, *Essentials of Materials Science and Engineering*. Thomson, Ontario, Canada, 2004.
- [15] S. Zhu, W. G. Fahrenholtz, G. E. Hilmas, and S. C. Zhang, "Pressureless sintering of carbon-coated zirconium diboride powders," *Materials Science and Engineering A* 459, 167-171 (2007).
- [16] Crystal and Ionic Radii of the Elements," p. F-175 in *CRC Handbook of Chemistry and Physics*, 62<sup>nd</sup> Edition, CRC Press, Boca Raton, FL (1981).
- [17] A. E. McHale (ed.) *Phase Diagrams for Ceramists*, Vol. X. American Ceramic Society, Westerville, OH, 1994, pp. 371.
- [18] David R. Clarke, "Interpenetrating Phase Composites" *J. Am. Ceram. Soc.*, 75 [4] 739-59 (1992).
- [19] H. O. Pierson, *Handbook of Refractory Carbides and Nitrides*, William Andrew Publishing/Noyes, Westwood, NJ, p. 68, 1996.
- [20] G. M. Song, Y.J. Wang and Y. Zhou, "Elevated temperature ablation resistance and Thermophysical properties of tungsten matrix composites reinforced with ZrC particles," *J. Mat. Sci.* 36, 4625-4631, (2001).

## SECTION

### 3. CONCLUSION

ZrC-W cermets were produced by conventional hot pressing as well as in situ reaction sintering. Cermets with ZrC contents of 35, 50 and 65 vol% were produced for both processing methods. For in situ reaction sintering, ZrO<sub>2</sub> and WC were reacted to form ZrC and W. The ZrC content was increased by adding extra C and/or ZrC to the reactants. The precursors were shown to fully react to form ZrC and W, which had a two phase, interpenetrating microstructure. Hardness was tested on all specimens produced. Strength was tested on the specimens containing 35 vol% ZrC. The materials showed promise for compositional flexibility, which leads to the ability to control the mechanical and physical properties by varying the ZrC:W ratio.

Composites containing 35 vol% ZrC were fully densified by both processing methods and then mechanical properties were tested. The specimens produced by reaction sintering were found to undergo substantial grain growth between 2050°C and 2100°C. The specimens sintered at 2050°C had an average feature size of less than 1 μm and a density of 98% while the specimens sintered at 2100°C had a feature size of 3 μm and a density of 97%. The properties of cermets with different feature sizes prepared by in situ reaction sintering were compared to the same composition prepared by hot pressing. The strength of the hot pressed specimen was the highest at 764 MPa. However, the reaction sintered specimen sintered at 2100°C had a higher hardness at 10 GPa compared to 9 GPa for the hot pressed specimen. The reaction sintered specimens are of interest for possible near-net shape fabrication. Of the two microstructures the smaller



features equated to a higher strength at 528 MPa compared to 448 MPa for the cermet sintered at the higher temperature. The larger feature size increased the fracture toughness, with a fracture toughness of  $8 \text{ MPa m}^{1/2}$  for the cermet sintered at  $2100^\circ\text{C}$  compared to  $7 \text{ MPa m}^{1/2}$  for the cermet sintered at  $2050^\circ\text{C}$ .

Further investigation on the control of the properties lead to the production of 50 vol% and 65 vol% ZrC additions. The specimens were made by in situ reaction sintering as well as hot pressing. The specimens made by hot pressing showed a decrease in the sintering temperature required for complete densification with increasing ZrC content. The specimens produced by reaction sintering had lower densities but showed promise for the production of fully dense materials.

The hardness was tested for the composition with different ZrC contents and showed a general increase with increasing ZrC content, with the reaction sintered specimens having slightly higher hardness values. However, the 65 vol% ZrC composition produced by in situ reaction sintering had a buildup of stresses that caused severe cracking which interfered with the hardness measurements, resulting in the hot pressed 65 vol% ZrC specimen having the highest measured hardness at 13 GPa compared to 9 GPa with 35 vol% ZrC prepared by hot pressing.

#### 4. SUGGESTIONS FOR FUTURE WORK

ZrC-W have shown promise as ultra-high temperature cermet materials. A better understanding of the relationship between the ZrC content, as well as the microstructure, and the properties could make this material attractive for many applications.

Cermets with different ratios of ZrC and W can be made by hot pressing. This method was used to produce materials for testing as a baseline for comparison to other ceramics made by in situ reaction sintering. To achieve ZrC additions greater than 35 vol%, the addition of C and/or ZrC can be used. Amounts lower than 35 vol% could be formed by adding additional W.

The full densification of higher amounts of ZrC will take adjustments to the powder processing and the sintering schedule. Charring the phenolic resin prior to pressing the pellets and adding a binder will reduce the volume change needed as well as reduce the risk of gas vent channels caused by the charring. Additionally, closer control of the furnace pressure and adjusting the holds so that the reaction happens in a controlled manner will also result in better densification.

The in situ reaction sintered specimen with 50 vol% ZrC was tested for strength which can be seen in Appendix A. The strength of 50 vol% ZrC is low compared to that of the 35 vol% ZrC. This is due to the lower relative density of the 50 vol% ZrC specimen used for strength testing, which was measured at 90% of the theoretical density. Improvements to the density of the 50 vol% ZrC specimen are needed in order to enable the use of the varying ratios of this material. Changing the ramp rates as well as extending the reaction holds will most likely have the greatest effect on increasing the

density. However, changes to the powder processing such as charring the phenolic resin after it is added to the powders and before pressing will reduce larger defects in the material and increase the strength. The knowledge gained from densifying the 50 vol% specimen can then be applied to produce specimens with 65 vol% ZrC.

Lastly the elevated temperature testing of these specimens is very important to the utilization of these materials in high temperature applications. Mechanical testing of the strength and fracture toughness with increasing temperature will give a better understanding of how these materials will form.

## APPENDIX

### 1. INTRODUCTION

The mechanical properties of 50 vol% ZrC were investigated to compare to the mechanical properties of 35 vol% ZrC. The resulting 50 vol% material had a lower strength that was low attributed to the low relative density (~90%) of the larger specimens necessary to produce mechanical test specimens. The amount of porosity reduced the strength of the cermet.

### 2. PROCEDURE

A larger billet was pressed in a steel die, 2.54 cm by 5.72 cm. The billet was first pressed uni-axially to 3.4 MPa followed by cold isostatic pressing. The pellet was sintered at 2100°C. Bars for flexure strength measurements were prepared to the dimensions specified in ASTM standard C1161-02c for size A bars (25 mm by 2.0 mm by 1.5 mm). The strength was tested in four point bending using a screw driven load frame and a fully articulated four point bend fixture. Only two bars were tested.

### 3. RESULTS

The bars tested in flexure had a relative density of 90%. The increase in the size of the billet was not adjusted for in the sintering schedule. The resulting strength was 194 MPa with an elastic modulus of 317 GPa.

Table 3-1 shows a comparison of the cermet with 50 vol% ZrC with the cermet with 35 vol% ZrC. The low strength of the material with 50 vol% ZrC is attributed to the

lower relative density. The increase in porosity is also the cause of the lower elastic modulus. However, the hardness did increase with increased ZrC content to ~11 GPa.

Table 3-1: Mechanical properties of ZrC-W cermets prepared by in situ reaction sintering with 35 vol% ZrC and 50 vol% ZrC

Material	Relative Density (%)	Flexure Strength (MPa)	Elastic Modulus (GPa)	Hardness (GPa)
50 vol% ZrC	90	194	317	11.3
35 vol% ZrC	97	448±26	345±8	9.2

#### 4. FUTURE WORK

Future investigation of the in situ reaction sintering process to produce ZrC-W cermets with 50 vol% ZrC will first require the ability to produce larger specimens with near full density. The increase in density will require alterations to the processing method. Some of these changes could include charring the phenolic resin before pressing, which would require the addition of a binder to press green bodies from the charred powder. Another option would be to alter the charring schedule so that more time is allowed for the gas to be removed. Once a near full dense billet is produced, the strength of the material can be tested as well as fracture toughness by chevron notch methods.

## VITA

Melissa Marie Giles Craft began her University career studying Mechanical Engineering at University of Missouri - Rolla, graduating in May 2007 Cum Laude. In the spring semester of 2007, Melissa began her transition to Ceramics by working as an Undergraduate Research Assistant, preparing Ultra High Temperature Ceramic samples for mechanical tests.

The beginning of Melissa's graduate work coincided with the name change from UMR to Missouri University of Science and Technology. She served as a Graduate Research Assistant during her graduate education.

Melissa was supported from research grants from AFOSR and NSF working on ZrC-W cermets. The project started to advance the work done by Shi C. Zhang on the novel process of in situ reaction sintering. Curiosity lead to the discovery that sintering at 2050°C resulted in a similar final density as the specimens produced at 2100°C; however, sintering at the lower temperature resulted in a different size microstructure. This discovery lead to a new focus of her research and the investigation of property control by microstructure and ZrC content began. The research has resulted in the work for 2 publications and 3 presentations. After completion of her Master's degree requirements Melissa will be moving to Idaho Falls to work as a Quality Engineer for Bettis Labs, a branch of the Bechtel Marine Propulsion Corporation, to investigate possible improvements to the fuel processing of nuclear reactors and ways to implement these changes.